Natland, J.H., Dick H.J.B., Miller, D.J., and Von Herzen, R.P. (Eds.)
Proceedings of the Ocean Drilling Program, Scientific Results Volume 176

7. Sulfide Mineral Chemistry and Petrography and Platinum Group Element Composition in Gabbroic Rocks from the Southwest Indian Ridge[1]

D. Jay Miller[2,3] and Pablo Cervantes[2,3]

ABSTRACT

Ocean Drilling Program (ODP) Leg 176 built upon the work of ODP Leg 118 wherein the 500-m section that was sampled represented the most complete recovery of an intact portion of lower oceanic crust ever described. During Leg 176, we deepened Hole 735B to >1500 m below seafloor in an environment where gabbroic rocks have been tectonically exposed at the Southwest Indian Ridge. This new expedition extended the remarkable recovery (>85%) that allowed unprecedented investigations into the nature of the lower oceanic crust as a result of Leg 118. Sulfide mineral and bulk rock compositions were determined from samples in the 1000-m section of oceanic gabbros recovered during Leg 176. The sulfide assemblage of pyrrhotite, chalcopyrite, pentlandite, and troilite is present throughout this section, as it is throughout the 500-m gabbroic section above that was sampled during Leg 118. Troilite is commonly present as lamellae, and the only interval where troilite was not observed is from the uppermost 150 m of the section sampled during Leg 118, which is intensely metamorphosed. The common presence of troilite indicates that much of the sulfide assemblage from Hole 735B precipitated from a magmatic system and subsequently underwent low-temperature reequilibration. Evaluation of geochemical trends in bulk rock and sulfides indicates that the combined effects of olivine accumulation in troctolites and high pentland-

[1]Miller, D.J., and Cervantes, P., 2002. Sulfide mineral chemistry and petrography and platinum group element composition in gabbroic rocks from the Southwest Indian Ridge. *In* Natland, J.H., Dick, H.J.B., Miller, D.J., and Von Herzen, R.P. (Eds.), *Proc. ODP, Sci. Results,* 176, 1–29 [Online]. Available from World Wide Web: <http://www-odp.tamu.edu/publications/176_SR/VOLUME/CHAPTERS/SR176_07.PDF>. [Cited YYYY-MM-DD]
[2]Department of Geology and Geophysics, Texas A&M University, College Station TX 77845, USA.
[3]Ocean Drilling Program, Texas A&M University, 1000 Discovery Drive, College Station TX 77845-9547, USA.
Correspondence author: **miller@odpemail.tamu.edu**

Initial receipt: 24 August 2000
Acceptance: 17 December 2001
Web publication: 6 August 2002
Ms 176SR-009

ite to pyrrhotite ratios account for the sporadic bulk rock compositions high in Ni. Bulk rock and sulfide mineral geochemical indicators that are spatially coincident with structural and physical properties anomalies indicate a heretofore unrecognized lithologic unit boundary in this section. Platinum-group element (PGE) compositions were also determined for 36 samples from throughout the section that were recovered during Leg 176. Whereas most samples had low (<0.4 ppb) PGE concentrations, rare samples had elevated PGE values, but no unique common trend between these samples is evident.

INTRODUCTION

Ophiolites are believed to preserve pieces of ocean crust exhumed and emplaced on land; however, these are invariably dismembered and tectonically modified. Extrusive basalts and sheeted dike sequences of the ocean crust are fortuitously exposed in the walls of rift valleys at both fast- and slow-spreading oceanic ridges, but intact exposures of gabbro, interpreted from seismic modeling to comprise in excess of two-thirds of the oceanic crust, are exceedingly more rare. These circumstances conspire to make the origin of the lower oceanic crust one of the most enigmatic puzzles under investigation by earth scientists.

In 1997, Ocean Drilling Program (ODP) Leg 176 successfully deepened Hole 735B, at the Atlantis II Fracture Zone on the Southwest Indian Ridge (Fig. F1), from the 500-m depth cored 10 yr ago during Leg 118 to a total depth of 1508 m. The combined results of drilling during Legs 118 and 176 (Robinson, Von Herzen, et al., 1989; Dick, Natland, Miller, et al., 1999) provide us with the most complete, intact section of lower ocean crust ever sampled. The gabbroic ocean crust at this site consists of several intervals of primitive olivine gabbro and troctolite. Each of these intervals is composed of many smaller intrusions, but shipboard geochemical analysis of major element oxides indicate a series of cycles relating to major pulses of magma with coherent fractionation sequences (Dick, Natland, Miller, et al., 1999). As a complement to other mineral chemistry and crustal evolution studies undertaken by the shipboard science party and various shore-based researchers, this paper reports the results of an investigation into sulfide mineralization and the presence, or absence for the most part, of platinum-group elements (PGEs) in the gabbros from this location.

PGEs are chalcophile and siderophile and are known to commonly occur with sulfide minerals in natural rock systems (Naldrett, 1989). PGE-bearing phases have been reported from ophiolite complexes (Prichard et al., 1986; Ohnenstetter et al., 1991; Pederson et al., 1993) generally associated with sulfide minerals or disseminated chromite layers. Although reports of PGE concentrations in ophiolitic gabbroic rocks are rare (e.g., Lachize et al., 1991; Prichard and Lord, 1990), gabbroic rocks from the plutonic sequence near the fast-spreading ridge at Hess Deep contain as much as 7.4 ppb Pt, 3.5 ppb Pd, and 3.1 ppb Au (Prichard et al., 1996). Troctolites associated with the ultramafic section at Hess Deep contain significantly higher concentrations of noble metals (36 ppb Pt and 54 ppb Pd) (Prichard et al., 1996), but dislocation of the section between the sites where gabbro and ultramafic rocks were recovered makes establishing any cogent relationship tenuous. Little is known about differences in PGE concentrations between ocean crust formed at fast- and slow-spreading ridges because of the lack of sampled exposures.

F1. Satellite altimetry free-air gravity map, p. 12.

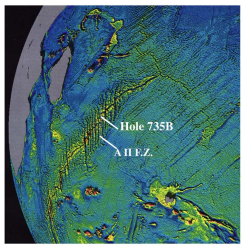

Igneous sulfides reported from the Leg 118 cores include pyrrhotite and chalcopyrite, with very rare pentlandite. Troilite is also present as a low-temperature exsolution product (Alt and Anderson, 1991; Natland et al., 1991). These sulfides are interpreted to have formed predominantly by accumulation of immiscible sulfide droplets. Although PGEs are efficiently scavenged from magmas by accumulation of immiscible sulfides, no systematic survey of PGE contents in the gabbros cored during Leg 118 has been reported.

This study was aimed at documenting the sulfide mineralogy and composition of gabbros recovered during Leg 176 in an effort to determine host phases of PGE mineralization in cores from Hole 735B, particularly to determine if PGE mineralization is hosted in primary magmatic phases or in secondary phases. Because of a strong alteration overprint, the only documented study of PGE mineralization in seafloor gabbros (Prichard et al., 1996) proved equivocal in determining whether PGE mineralization had been hosted in primary sulfides and reprecipitated as independent phases during alteration or if they were precipitated directly as independent phases. Given the overall extremely low levels of alteration in the gabbros from Hole 735B, we hoped to be able to see through any hydrothermal overprint and determine if platinum-group minerals (PGMs) are preserved as primary phases. Although PGE concentrations in oceanic gabbros may be low, the vast amount of ocean crust requires research into the distribution of highly refractory chalcophile elements to evaluate the global PGE budget and determine how PGEs are extracted from the mantle and concentrated in the ocean crust.

GEOLOGIC SETTING AND LITHOSTRATIGRAPHY

Hole 735B is located on a ~200-km-long transverse ridge along the eastern wall of the Atlantis II transform valley (Fig. F1). This hole is on the south end of a steep-sided, flat-topped bank, roughly 9 km north-to-south by 4 km east-to-west, that rises some 5 km above the transform valley floor (Fig. F2). See the Leg 176 *Initial Reports* volume and references therein for complete documentation of the tectonic setting of the Atlantis II bank (Dick, Natland, Miller, et al., 1999). The shipboard science party documented 457 igneous intervals and six major lithostratigraphic units during the Leg 176 description process (Fig. F3).

METHODS

In the first-pass petrographic study, 85 polished thin sections were prepared and examined from samples selected aboard the *JOIDES Resolution* with an eye toward locating intervals of sulfide concentration or abundance coincident with other petrological markers, specifically indicators of primitive magmas, that are the most likely host of primary PGE-bearing minerals. Many thin sections were effectively barren, despite observation of sulfide in the sample slab; commonly, only one or two grains were present. A subset of 25 samples that had the most abundant igneous textured sulfides was selected. In addition, a review of pathfinder elements in bulk-rock chemical analyses suggested that another 11 samples had higher than average Cu and Ni compositions. Most of the oxide gabbros (from more evolved magmas) contained a mineral assemblage wherein pyrite was the major, if not the only sul-

F2. Three-dimensional shaded-relief image, p. 13.

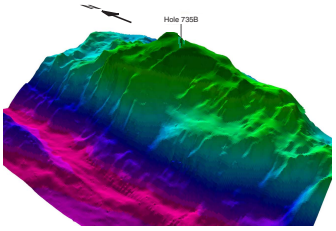

F3. Bulk rock Mg number vs. depth of gabbroic rocks, p. 14.

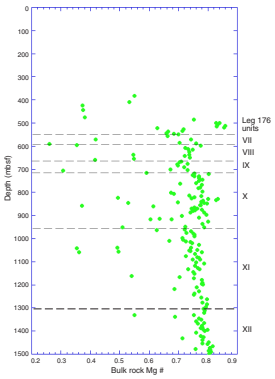

fide phase present. Only the oxide-bearing gabbros with elevated pathfinder element bulk-rock compositions were included in further study. A total of 36 samples were pulverized and sent to Commonwealth Scientific and Industrial Research Organization (CSIRO) Exploration and Mining, North Ryde New South Wales, Australia, for PGE analysis by inductively coupled plasma–mass spectrometry (ICP-MS). Pt, Pd, Ru, and Ir were calibrated by isotope dilution. Rh and Au were determined by external calibration. Analytical methods are detailed in Evans et al. (1993). Petrographic descriptions of these samples are summarized in Table **T1.**

T1. Petrographic summaries, p. 24.

Sulfide mineral chemistry was determined by electron microprobe on the Texas A&M Department of Geology and Geophysics Cameca SX-50 Superprobe using a combination of glass, mineral, and pure metal standards. Since this instrument is equipped with an ultrathin rather than a beryllium window, we were able to acquire high resolution on all peaks of interest using an accelerating voltage of 15 KeV. Count times were 20 to 30 s with a 1-µm-wide beam.

Bulk rock chemistries were determined by $LiBO_2$ fusion followed by inductively coupled plasma (ICP) spectrometry. Major element oxides were determined by ICP–atomic emission spectrometry and trace elements by ICP-MS. These analyses were performed by Acme Analytical Laboratories, Vancouver, British Columbia, Canada. Replicate samples and U.S. Geological Survey standard reference materials were included in the analytical suite as unknowns to ensure accuracy and precision.

RESULTS

Sulfide Mineralogy

As in the cores recovered during Leg 118, the most common sulfides present in the cores from the lower two-thirds of Hole 735B are globular igneous sulfides, although every thin section examined contains secondary sulfides in subordinate amounts. In this sample suite, the abundance of sulfide does not correlate with depth or with any specific lithology; however, this may be an artifact of sampling, as only the most sulfide-rich samples were collected. Unlike the cores from Leg 118, no obvious intervals are devoid of or significantly poorer in sulfide mineralization, although this might be expected because >70% of the material recovered is relatively fresh olivine gabbro.

Sulfide mineralization was subdivided into groups based on the three most common assemblages:

1. Armored (completely encased in a silicate phase in the two dimensions visible on the surface of the thin section), irregular to rounded or oblong, generally multiphase globules ranging from a few tens to a few hundred micrometers across, without reaction coronas;
2. Similarly shaped and sized globules hosted in brown amphibole, commonly, but not exclusively, at the contact between fresh igneous phases; and
3. Subrectangular to angular, predominantly single-phase small grains, as inclusions along cleavage and fractures, in stringers, and interstitial to and intermixed with alteration halos around fresh igneous phases.

The third group, although generally the least abundant, was present in every section examined and probably represents secondary mineralization. The sulfides armored in plagioclase or pyroxene are the next most common morphology in terms of the number of thin sections where they were recognized, but sulfides armored in olivine are exceedingly rare. More common in terms of sheer numbers of occurrence, however, are the sulfides that are present in association with translucent brown amphibole.

Pyrrhotite is far and away the most common igneous sulfide phase and is present in every sample examined that contained igneous sulfide. In order of greatest to least abundance, other sulfide phases identified are chalcopyrite, pentlandite, troilite, sphalerite, and galena. Pyrite is the most common secondary sulfide phase. The most common association, seen in cores from throughout Hole 735B, is pinkish tan (in reflected light), pyrrhotite with blades of brassy yellow chalcopyrite.

Monomineralic grains of pyrrhotite are common; single-phase chalcopyrite grains are less so. The association of pyrrhotite, chalcopyrite, pentlandite, and troilite was reported in Cores 118-735B-45R, 54R, 68R, and 81R (216, 258, 335, and 434 meters below seafloor [mbsf], respectively) (Alt and Anderson, 1991). Intergrowths of these four phases were common throughout the cores recovered during Leg 176 but were significantly more abundant in sections containing fresh olivine (Fig. **F4**). Review of thin sections from Leg 118 indicates that this four-phase intergrowth is also present in Cores 118-735B-21R, 27R, 31R, and 34R (89, 122, 143, and 158 mbsf, respectively). Again, all of these samples are fresh olivine gabbro. Where present, the largest part of these multiphase grains is (in reflected light) pinkish tan pyrrhotite with faint, zigzag-shaped lamellae of lighter-hued troilite (Fig. **F5**). Pentlandite is light cream yellow and usually is present in one or two discrete patches with sharp, irregular margins. Brassy yellow chalcopyrite is present in blades and blebs. The troilite lamellae end abruptly at the contact with either pentlandite or chalcopyrite and do not taper to a fine point as these lamellae do when hosted only in pyrrhotite. Troilite was not seen in samples that contained only pyrrhotite or only pyrrhotite and chalcopyrite. In rare samples, troilite is significantly more abundant than pyrrhotite (Fig. **F4**).

Sulfide Mineral Chemistry

Table **T2** contains average sulfide mineral compositions from samples throughout the recovered section. These averages represent three to seven analyses per grain, and five to 10 grains per sample. Pyrrhotite is present in every sample analyzed. From 500 to 1165 mbsf, all samples analyzed are stoichiometrically close to Fe_7S_8 and contain from 0.2 to 0.9 wt% Ni. Between 1165 and 1195 mbsf, there is a radical change in the composition of the sulfides from predominantly pyrrhotite (Fig. **F6**) to approaching stoichiometric troilite, with all samples containing less than 0.5 wt% Ni (Fig. **F7**). No unit boundary was identified at this location during Leg 176; however, at this depth there is a radical drop in magmatic foliation intensity, concomitant with a sharp decrease in crystal-plastic foliation and a major reduction in bulk magnetic susceptibility (Dick, Natland, Miller, et al., 1999). With an eye of faith, there appears to be a shift in the trend of Mg number at this depth (Fig. **F3**), suggesting with the data above that there may be a lithologic boundary at this depth.

F4. Multiphase sulfide globule, Sample 176-735B-123R-4, 106–111 cm, p. 15.

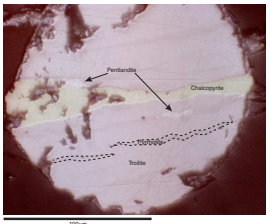

F5. Multiphase sulfide grain, Sample 176-735B-185R-3, 121–126 cm, p. 16.

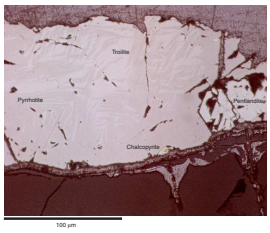

T2. Sulfide mineral analyses, p. 26.

F6. Fe in pyrrhotite, p. 17.

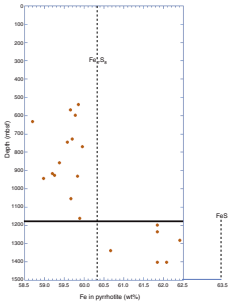

F7. Ni in pyrrhotite, p. 18.

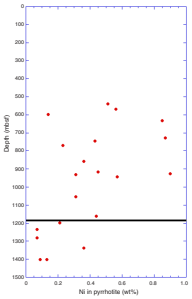

Pentlandite (stoichiometrically $[Fe,Ni]_9S_8$) compositions are variable downsection, but discounting the shallowest sample analyzed, Ni composition is relatively constant (Fig. F8) at about 29 wt% (±2 wt%). Co in pentlandite ranges from 3 to ~14 wt% (Fig. F9), substituting for Fe. There appears to be a rapid increase in Co in pentlandite at the base of the lithologic unit boundary at ~960 mbsf (see Fig. F3) and a steady decrease in Co below the proposed lithologic boundary between 1165 and 1190 mbsf.

Chalcopyrite is stoichiometric in all samples but contains as much as 1.15% wt% Zn in solid solution.

F8. Ni in pentlandite, p. 19.

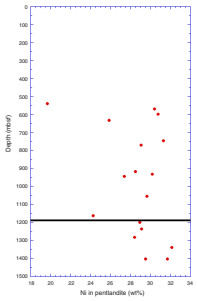

F9. Co in pentlandite, p. 20.

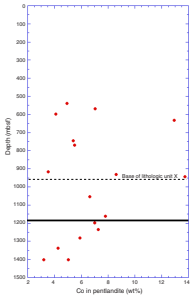

Silicate Mineralogy

The primary mineralogy of the samples described consists of plagioclase, clinopyroxene, and olivine, which are present in nearly all of the samples, with orthopyroxene and amphibole scattered irregularly throughout the section. Plagioclase mode percent ranges between 35% and ~80%, with most of the samples ranging between 40% and 60%. Clinopyroxene ranges between 1.6% and 57%, most commonly in the range of 20% to 40%. Olivine mode ranges from nil to >50%, but generally falls between 2% and 20%. Brown amphibole (possibly igneous) is present in 28 of the samples described in this study and varies between 0.1% and 4.9% of the mode. The average proportions of olivine, clinopyroxene, and plagioclase are consistent with the cotectic proportions of these phases in the 2-kbar crystallization experiments of Grove et al. (1992) on mid-ocean-ridge basalt.

Alteration is variable and ranges from <1% to >55%. Most of the samples we looked at, however, are <10% altered. Of the primary minerals in this suite, olivine consistently shows the highest degree of alteration and is altered to amphibole, talc, smectite, and magnetite in variable proportions. Clinopyroxene is altered to amphibole. Plagioclase, although apparently the least altered primary phase, is in places replaced by secondary feldspar, actinolite, and chlorite; the last two alteration phases are particularly common where plagioclase abuts either clinopyroxene or olivine.

DISCUSSION

According to Craig and Kullerud (1969), the sulfide assemblage of pyrrhotite, chalcopyrite, troilite, and pentlandite is typical of igneous sulfides segregated from mafic magmas that subsequently underwent lower temperature reequilibration. The presence of troilite, which is not commonly reported in mafic igneous rocks but which is present throughout the entire section sampled during both Legs 118 and 176 (with the exception of the upper 150 m or so), indicates that the pyrrhotite was originally quite Fe rich and underwent exsolution at low temperature (Kissin and Scott, 1982) to troilite plus pyrrhotite. Toulmin and Barton (1964) argue that troilite exsolution from Fe-rich pyrrhotite indicates lower sulfur fugacity than in assemblages that contain only relatively Fe-poorer pyrrhotite; however, in these samples troilite is present, associated with both Fe-rich and Fe-poor pyrrhotite (see Figs. F4, F5).

One method used in this investigation to target sulfide-bearing intervals that might contain PGE was to identify intervals that show anomalously high values of pathfinder elements that have partitioning

behavior similar to PGE. Figure F10 illustrates the concentration with depth in the core of two of the most useful of these pathfinder elements, Cu and Ni. Cu and Ni are both chalcophile and siderophile, partitioning strongly into sulfide phases in a magmatic system. Most of these data are from the shipboard data sets of Legs 118 and 176 (Robinson, Von Herzen, et al., 1989; Dick, Natland, Miller, et al., 1999). New bulk chemical analyses resulting from this study are presented in Table T2. Ni and Cu average 110 and 65 ppm, respectively, throughout the section, and both show an overall slight increase in concentration with depth.

Ni concentration relative to depth shows many more high-concentration spikes than does Cu. There are two possible explanations for this phenomenon. Figure F11 is a plot of bulk rock Ni and Cu for all analyses available from Hole 735B. These have been subdivided into oxide-bearing gabbros, gabbros, and olivine gabbros, based on petrography. All oxide-bearing gabbros, regardless of grain size or olivine content, have been grouped together for this illustration. Virtually all of the oxide-bearing gabbros show depleted Ni contents at any given Cu content. Presumably this is because these gabbros precipitated from differentiated liquids where olivine had sequestered most of the available Ni. The gabbros and olivine-bearing gabbros show a pattern with coincident increase in Cu and Ni but substantial variability. In some of the samples, Ni values above the generally increasing Cu-Ni line can be attributed to olivine accumulation. Average Ni abundance in olivine reported from Leg 118 postcruise research (Ozawa et al., 1991) is 100 to 300 ppm in gabbros and oxide-bearing gabbros but exceeds 1500 ppm in troctolites. Where the modal olivine abundance in troctolites approaches 50%, high bulk rock Ni contents are possible. In all the samples examined from the Leg 176 suite, however, it appears that in each case the high bulk Ni compositions are due to a marked change in the ratio of pentlandite to pyrrhotite in the sulfide assemblage. In general, pentlandite comprises <10% of the total sulfide minerals (see Figs. F4, F5). In each interval where there is a high Ni concentration, the proportion of pentlandite increases, with pentlandite accounting for as much as 90% of the sulfide mineral assemblage (Fig. F12). Pentlandite in these samples contains >30 wt% Ni, and this can account for enrichments as high as 800 ppm in bulk Ni composition.

Cu and Ni bulk concentrations also mimic lithostratigraphic variation based on magnesium number (compare Figs. F3 and F10). The variability of Cu and Ni concentration is fairly constant below 500 mbsf, except in the interval from 960 to 1170 mbsf, where compositional range is very limited. As noted earlier, the lower contact of this interval is coincident with a major shift in pyrrhotite composition, a sharp decrease in magmatic foliation, and a sharp decrease in magnetic susceptibility (Dick, Natland, Miller, et al., 1999). All of these indicate that the gabbroic rock below 1170 mbsf precipitated from a different magma batch than the gabbro that is higher upsection.

In those sulfides analyzed by electron microprobe, pentlandite is the host for nearly all of the detectable Ni and Co. According to Mazdab and Force (1998), comparison of Co/Ni ratios in sulfides readily differentiate Fe oxide deposits (Co/Ni > 1) from magmatic Fe-Ti oxide or magmatic immiscible sulfide Ni-Fe-Cu systems (Co/Ni < 1). All samples in this study have a Co/Ni > 1, indicating that they are magmatic.

Although the initial focus of this investigation was PGE mineralization, only a few of the samples analyzed proved to have concentrations above a background of ~0.4 ppb total PGE and Au (Table T3). Concen-

F10. Plots vs. depth of bulk rock Ni and Cu compositions, p. 21.

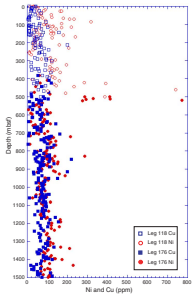

F11. Covariation of bulk rock Ni and Cu, p. 22.

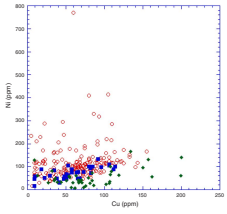

F12. Pentlandite and pyrrhotite, Sample 176-735B-123R-4, 106–111 cm, p. 23.

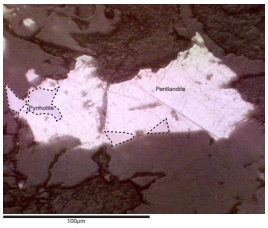

T3. Bulk rock chemistry, p. 27.

trations significantly higher than this background value are present in the interval between 500 and 520 mbsf, and 744, 1192, and 1430 mbsf. The only petrographic or geochemical similarity among these samples is the presence of pentlandite with pyrrhotite and chalcopyrite. These samples do not have universally distinct proportions of these phases, and several other samples have this sulfide assemblage and do not have elevated PGE. However, each of these samples does have distinct characteristics from the routine gabbro sampled in Hole 735B. The interval between 500 and 520 mbsf (Samples 176-735B-90R-1, 123–125 cm; 90R-4, 42–45 cm; 90R-6, 72–77 cm; and 176-735B-91R-1, 106–111 cm) all have much higher than average bulk Ni composition and contain more abundant pentlandite than most of the samples examined. The sample from 744 mbsf (Sample 176-735B-123R-4, 106–111 cm) has the highest analyzed value of Pd and contains no detectable Pt. This sample contains armored polyphase sulfide globules with the most convincing igneous textures observed (see Fig. F4). Another petrographic distinction of this sample is that throughout the section there is, in general, an antithetic relationship between the abundances of olivine and sulfide phases. As the amount of olivine increases, the abundance of primary sulfide minerals declines. This sample, however, contains both abundant olivine and a relatively high abundance of sulfide minerals. Shipboard core descriptions (Dick, Natland, Miller, et al., 1999) identified this interval as a microgabbro, rich in olivine and sulfides, with an intrusive contact with the surrounding pegmatitic-textured gabbro. Although structurally a late intrusive event, based on the abundance of olivine and primary sulfides, this interval must represent a relatively primitive magma. The sample from 1192 mbsf (Sample 176-735B-175R-1, 115–120 cm) is coincident with the geochemical boundary marked by the radical change in primary sulfide composition. The sample from 1430 mbsf (Sample 176-735B-203R-1, 11–13 cm) is from a 6-cm-thick chalcopyrite-, pentlandite-, and pyrrhotite-bearing clinopyroxenite and contains the highest abundance of PGE detected. A thin section from this sample was examined in an exhaustive search under reflected light at high magnification with a petrographic microscope and with backscatter electron imaging on the electron microprobe, and no platinum-group element–bearing minerals were detected. However, all of the PGEs in this sample, if concentrated in a single grain, would require that the grain be only a few micrometers across.

SUMMARY

This investigation can be summarized as follows:

1. The common presence of troilite throughout the entire section that was sampled during both Legs 118 and 176 indicates that much of the sulfide assemblage from Hole 735B precipitated from a magmatic system and subsequently underwent low-temperature reequilibration.
2. The only interval where troilite was not identified is the intensely foliated and metamorphosed upper 150 m of the section (0–150 mbsf). Although the available thin section suite from this part of the section is incomplete, armored, globular sulfides were exceedingly rare.
3. Troilite is present with both Fe-rich and Fe-poor pyrrhotite compositions but does not occur in this sample suite unless pyrrho-

tite, chalcopyrite, and pentlandite are also present. Samples with only pyrrhotite or pyrite do not contain troilite.

4. The combined effects of olivine accumulation in troctolites and high pentlandite to pyrrhotite ratios accounts for the sporadically high bulk-rock Ni compositions.
5. The lower variability of Ni and Cu bulk-rock compositions between 960 and 1170 mbsf and the coincidence of the lower part of this interval with a change in pyrrhotite composition, a sharp decrease in magmatic foliation, and a sharp decrease in magnetic susceptibility suggest a different magma batch below and above.
6. The Co/Ni value of the sulfides examined in this study suggests that they were formed in a magmatic Fe-Ti oxide or magmatic immiscible sulfide Ni-Fe-Cu system. The reader should note, however, that the sample suite for this study was heavily biased away from oxide-bearing intervals, and the sulfides in the oxide-bearing intervals may have a completely different composition and paragenesis.
7. PGE concentrations are low in all samples investigated, with a background value of <0.4 ppb. Rare samples have elevated values, but there is no evident commonality in occurrence. The highest values analyzed are from a thin sulfide-bearing clinopyroxenite near the bottom of the section.

ACKNOWLEDGMENTS

The authors wish to thank the Ocean Drilling Program for providing the samples for this investigation. ODP is sponsored by the U.S. National Science Foundation (NSF) and participating countries under management of Joint Oceanographic Institutions (JOI), Inc. Funding for this research was provided by United States Science Advisory Committee (USSAC) and NSF.

We thank Ray Guillemette for his assistance with the electron microprobe and Noreen Evans of the Commonwealth Scientific and Industrial Research Organization (CSIRO) for the PGE analyses. The manuscript benefitted from reviews by Jamie Allan, Rob Zierenberg, and Jim Natland, and we thank them all for their input. This research was supported by USSSP grant #418925.

REFERENCES

Alt, J.C., and Anderson, T.F., 1991. Mineralogy and isotopic composition of sulfur in layer 3 gabbros from the Indian Ocean, Hole 735B. *In* Von Herzen, R.P., Robinson, P.T., et al., *Proc. ODP, Sci. Results,* 118: College Station, TX (Ocean Drilling Program), 113–126.

Craig, J.R., and Kullerud, G., 1969. Phase relations in the Cu-Fe-Ni-S system and their application to magmatic ore deposits. *In* Wilson, H.D.B. (Ed.), *Magmatic Ore Deposits: A Symposium*. Econ. Geol. Monogr., 4:344–358.

Dick, H.J.B., Meyer, P.S., Bloomer, S., Kirby, S., Stakes, D., and Mawer, C., 1991. Lithostratigraphic evolution of an in situ section of oceanic layer 3. *In* Von Herzen, R.P., Robinson, P.T., et al., *Proc. ODP, Sci. Results,* 118: College Station, TX (Ocean Drilling Program), 439–540.

Dick, H.J.B., Natland, J.H., Miller, D.J., et al., 1999. *Proc. ODP, Init. Repts.,* 176 [CD-ROM]. Available from: Ocean Drilling Program, Texas A&M University, College Station, TX 77845-9547, U.S.A.

Evans, N.J., Gregoire, D.C., Grieve, R.A.F., Goodfellow, W.D., and Veizer, J., 1993. Use of platinum-group elements for impactor identification: terrestrial impact craters and Cretaceous-Tertiary boundary. *Geochim. Cosmochim. Acta,* 57:3737–3748.

Grove, T.L., Kinzler, R.J., and Bryan, W.B., 1992. Fractionation of mid-ocean ridge basalt (MORB). *In* Morgan, J.P., Blackman, D.K., and Sinton, J.M. (Eds.), *Mantle Flow and Melt Generation at Mid-Ocean Ridges*. Geophys. Monogr., Am. Geophys. Union, 71:281–310.

Kissin, S.A., and Scott, S.D., 1982. Phase relations involving pyrrhotite below 350°C. *Econ. Geol.,* 77:1739–1754.

Lachize, M., Lorand, J.P., and Juteau, T., 1991. Cu-Ni-PGE magmatic sulfide ores and their host layered gabbros in the Haymiliyah fossil magma chamber (Haylayn block, Semail Ophiolite nappe, Oman). *In* Peters, T., Nicolas, A., and Coleman, R.J. (Eds.), *Ophiolite Genesis and Evolution of the Oceanic Lithosphere*. Petrol. Struct. Geol., 5:209–229.

Mazdab, F.K., and Force, E.R., 1998. Comparison of cobalt and nickel contents in sulfides from iron-oxide (Cu-Au-U-REE) occurrences with other hydrothermal and magmatic systems. *Abstr. Annu. Meet., Geol. Soc. Am.,* 30:369. (Abstract).

Naldrett, A.J., 1981. Platinum-group element deposits. *In* Cabri, L.J. (Ed.), *Platinum Group Elements: Mineralogy, Geology, Recovery*. Spec. Vol.—Can. Inst. Min. Metall., 23:197–231.

————, 1989. *Magmatic Sulphide Deposits*. Oxford Monogr. Geol. Geophys., 14.

Natland, J.H., Meyer, P.S., Dick, H.J.B., and Bloomer, S.H., 1991. Magmatic oxides and sulfides in gabbroic rocks from Hole 735B and the later development of the liquid line of descent. *In* Von Herzen, R.P., Robinson, P.T., et al., *Proc. ODP, Sci. Results,* 118: College Station, TX (Ocean Drilling Program), 75–111.

Ohnenstetter, M., Karaj, N., Neziraj, A., Johan, Z., and Cina, A., 1991. Le potentiel platinifère des ophiolites: minéralisations en éléments du groupe du platine (PGE) dans les massifs de Tropoja et Bulqiza, Albanie. *C. R. Acad. Sci. Ser. 2,* 313:201–208.

Ozawa, K., Meyer, P.S., and Bloomer, S.H., 1991. Mineralogy and textures of iron-titanium oxide gabbros and associated olivine gabbros from Hole 735B. *In* Von Herzen, R.P., Robinson, P.T., et al., *Proc. ODP, Sci. Results,* 118: College Station, TX (Ocean Drilling Program), 41–73.

Pedersen, R.B., Johannesen, G.M., and Boyd, R., 1993. Stratiform PGE mineralisations in the ultramafic cumulates of the Leka ophiolite complex, central Norway. *Econ. Geol.,* 88:782–803.

Prichard, H.M., and Lord, R.A., 1990. Platinum and palladium in the Troodos ophiolite complex, Cyprus. *Can. Mineral.,* 28:607–617.

Prichard, H.M., Neary, C.R., and Potts, P.J., 1986. Platinum-group minerals in the Shetland Ophiolite. *In* Gallagher, M.J., Ixer, R.A., Neary, C.R., and Prichard, H.M.

(Eds.), *Metallogeny of Basic and Ultrabasic Rocks*. London Inst. Min. Metall. Monogr., 395–414.

Prichard, H.M., Puchelt, H., Eckhardt, J.-D., and Fisher, P.C., 1996. Platinum-group-element concentrations in mafic and ultramafic lithologies drilled from Hess Deep. *In* Mével, C., Gillis, K.M., Allan, J.F., and Meyer, P.S. (Eds.), *Proc. ODP, Sci. Results,* 147: College Station, TX (Ocean Drilling Program), 77–90.

Robinson, P.T., Von Herzen, R., et al., 1989. *Proc. ODP, Init. Repts.,* 118: College Station, TX (Ocean Drilling Program).

Toulmin, P., and Barton, P.B., 1964. A thermodynamic study of pyrite and pyrrhotite. *Geochim. Cosmochim. Acta,* 28:641–671.

Figure F1. Satellite altimetry free-air gravity map showing the Southwest Indian Ridge, the Atlantis II Fracture Zone (AII FZ), and the location of Hole 735B.

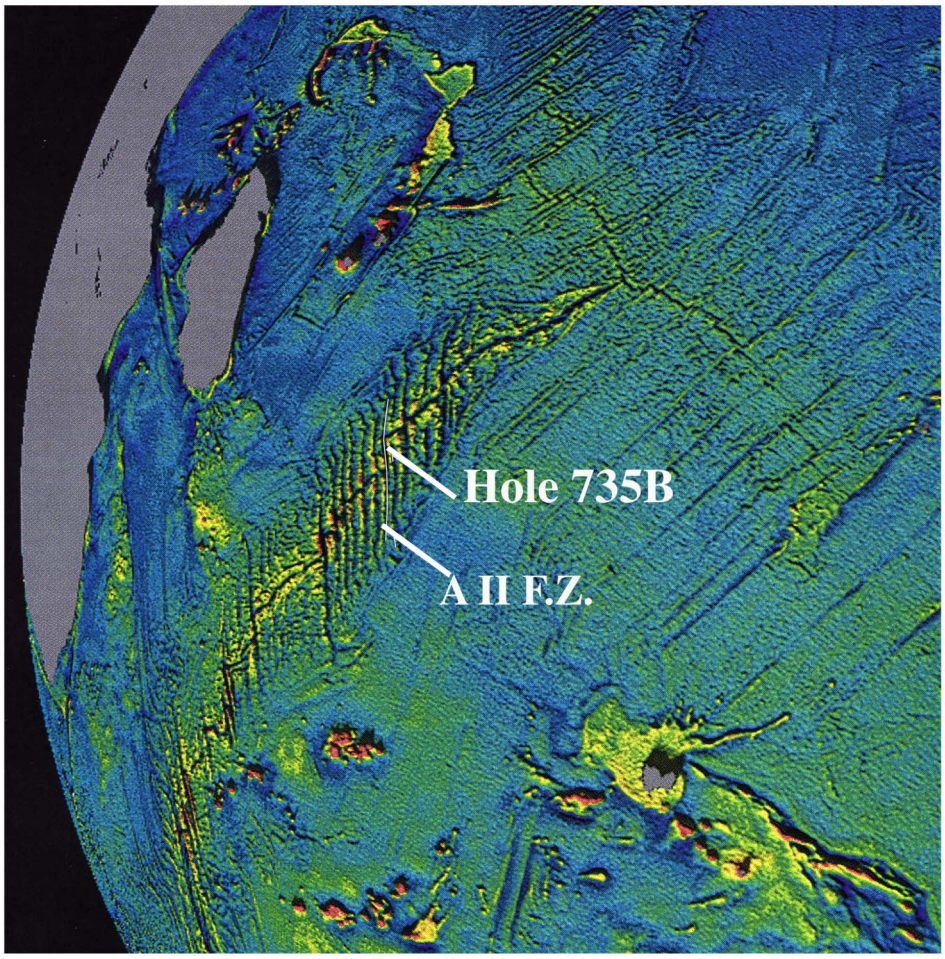

Figure F2. Three-dimensional shaded-relief image of the Atlantis Bank (looking northeast) along the wall of the Atlantis II transform fault (data from Dick et al., 1991). The image shows the location of Hole 735B drilled during Legs 118 and 176. The image shows the transform valley, transverse ridges with the Atlantis Bank (highest region), and the termination of the median tectonic ridge in the axis of the transform valley.

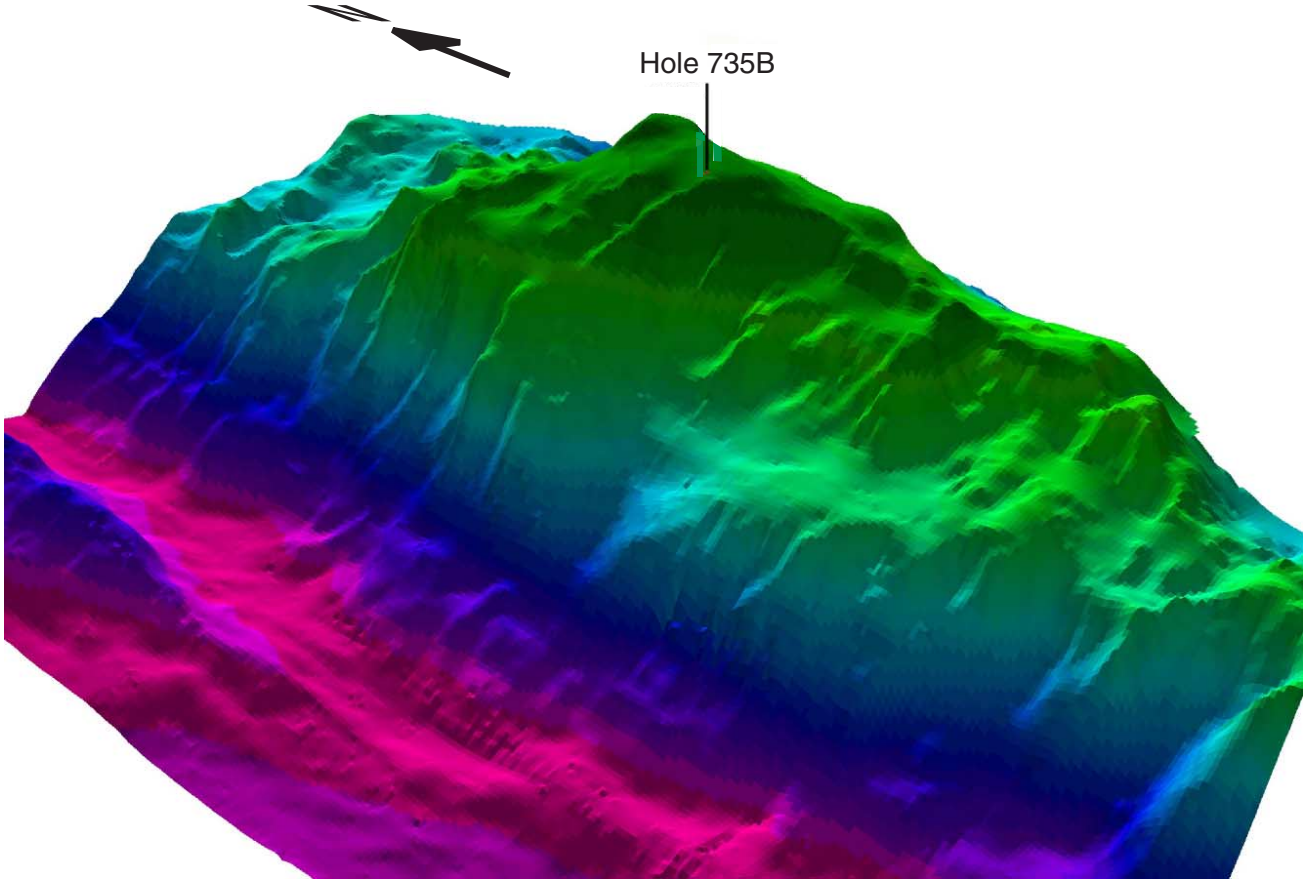

Figure F3. Bulk rock Mg number vs. depth of gabbroic rocks from Hole 735B analyzed during Leg 176 (Dick, Natland, Miller, et al., 1999). Roman numerals indicate the lithostratigraphic units defined during the cruise. The light dashed lines show the locations of unit contacts.

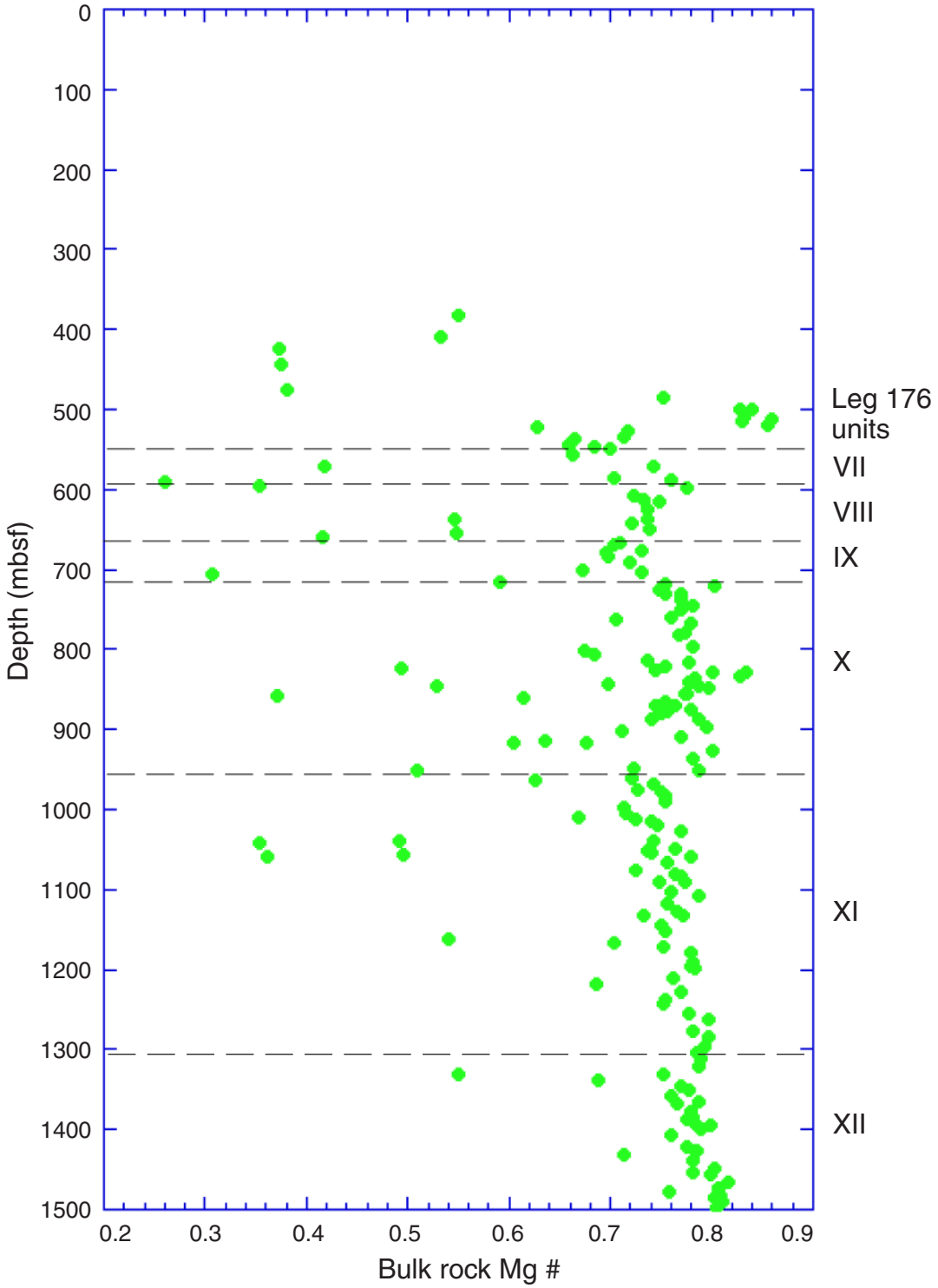

Figure F4. Multiphase sulfide globule in Sample 176-735B-123R-4, 106–111 cm (744 mbsf). Troilite is the most abundant phase in this sample of Fe-poor pyrrhotite. The dashed line highlights a darker-hued pyrrhotite lamellae; several other subparallel but irregular lamellae are apparent.

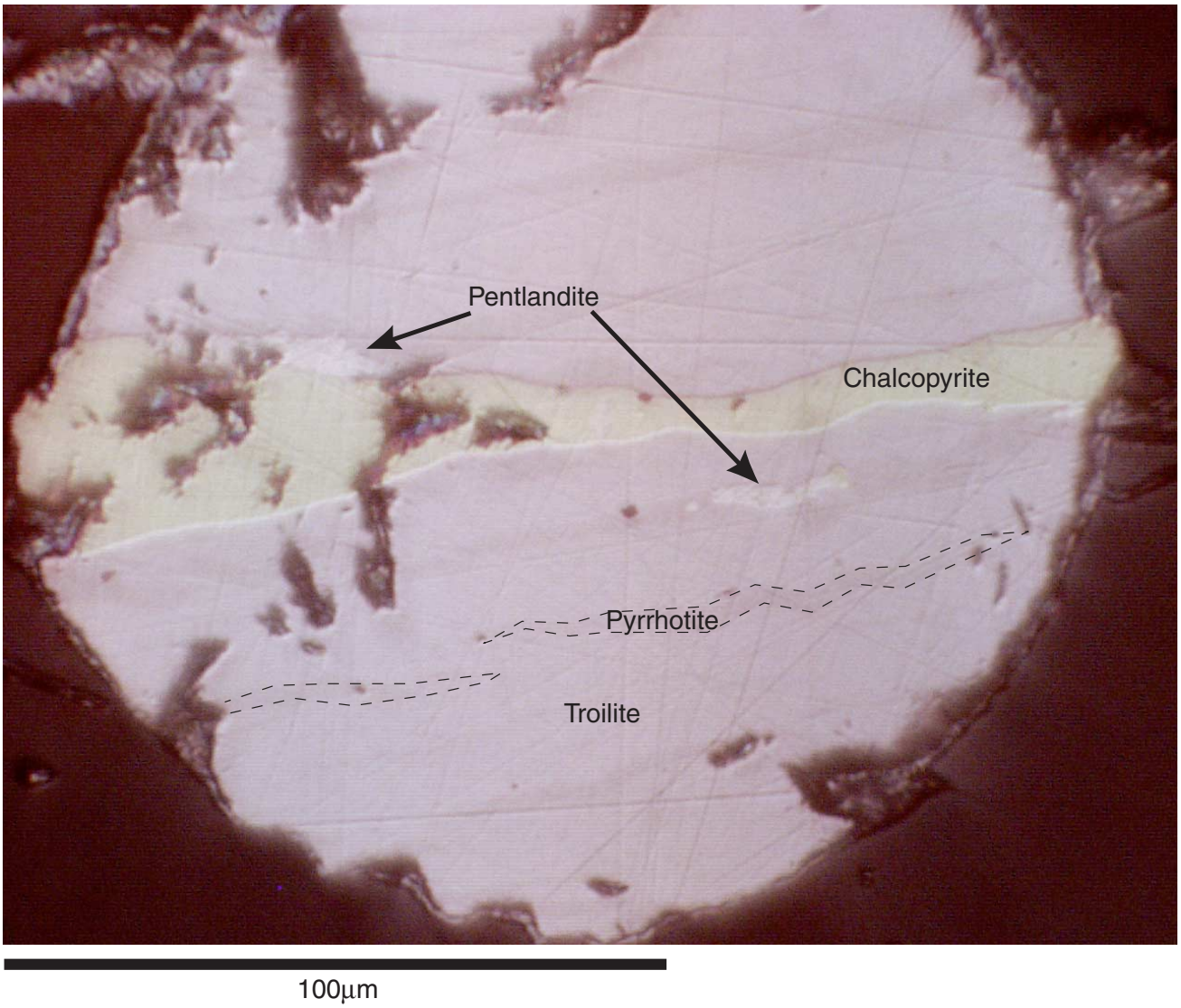

Figure F5. Multiphase sulfide grain with relatively Fe-rich pyrrhotite in Sample 176-735B-185R-3, 121–126 cm (1282 mbsf).

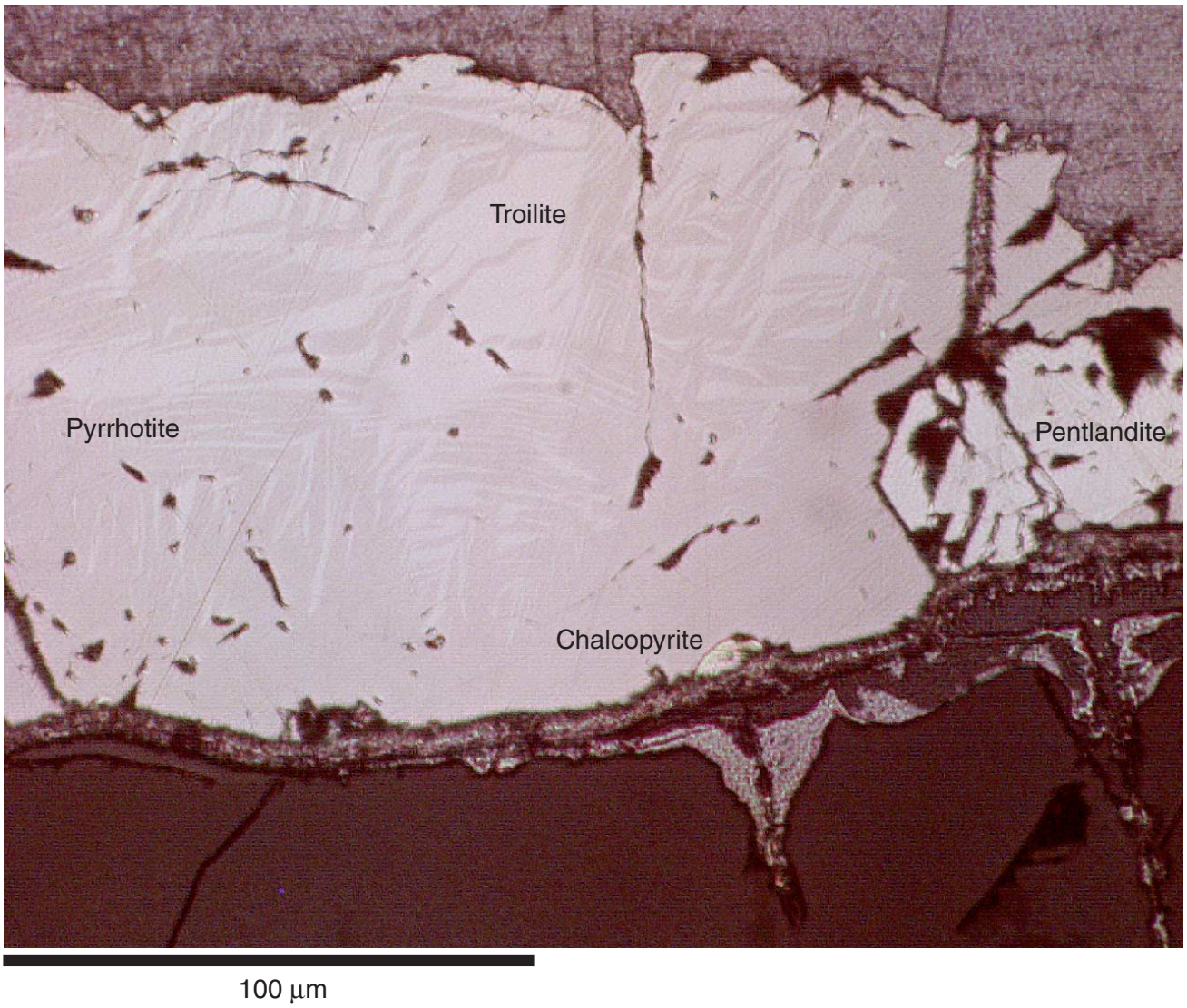

Figure F6. Fe in pyrrhotite shows a radical change in composition between 1165 and 1200 mbsf from Fe-poor to Fe-rich varieties (stoichiometric pyrrhotite to nearly troilite). The dark horizontal line marks the depth of this abrupt mineralogical and geochemical boundary.

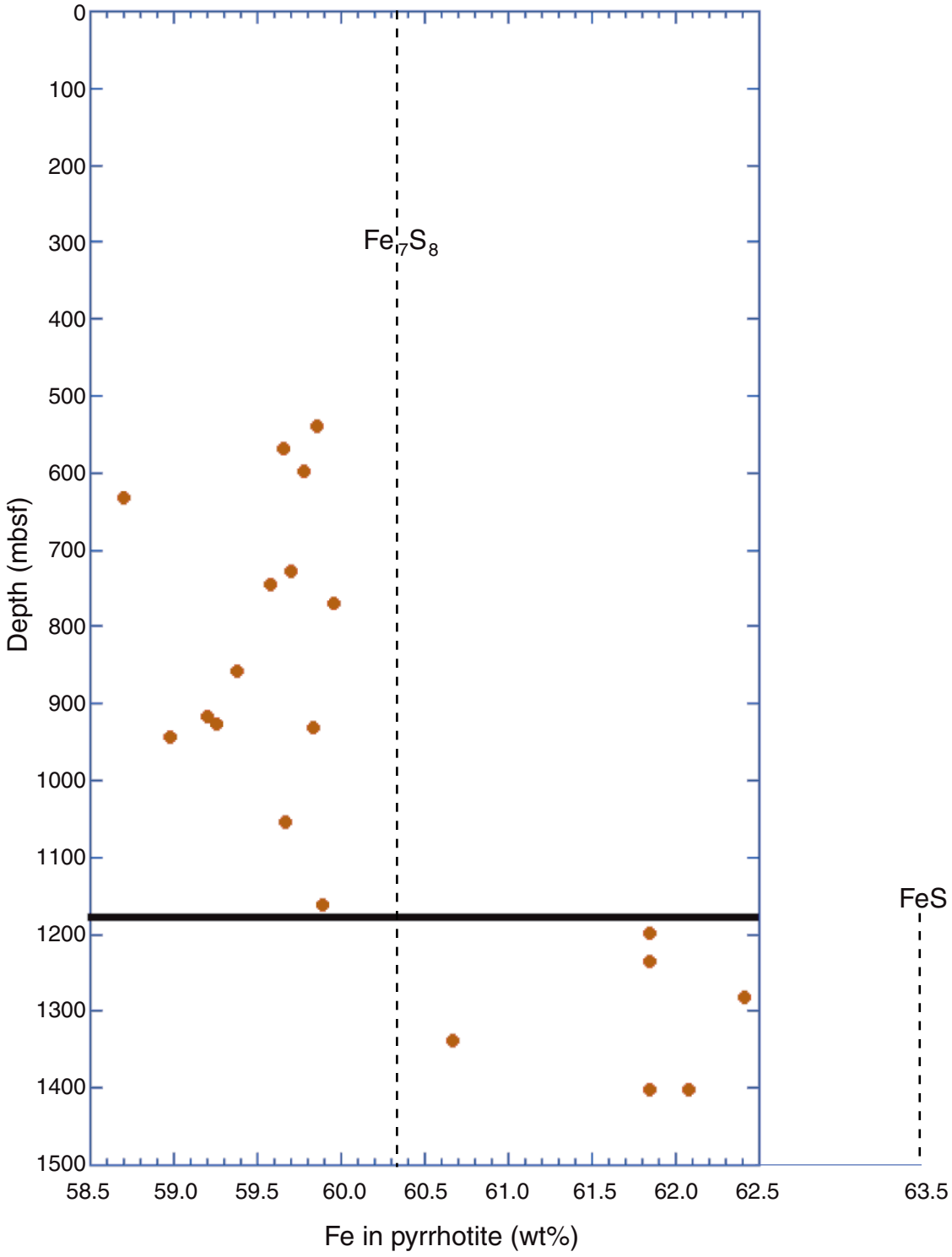

Figure F7. Ni in pyrrhotite shows a sharp decrease coincident with the change in Fe composition. The dark horizontal line marks the depth of this abrupt mineralogical and geochemical boundary.

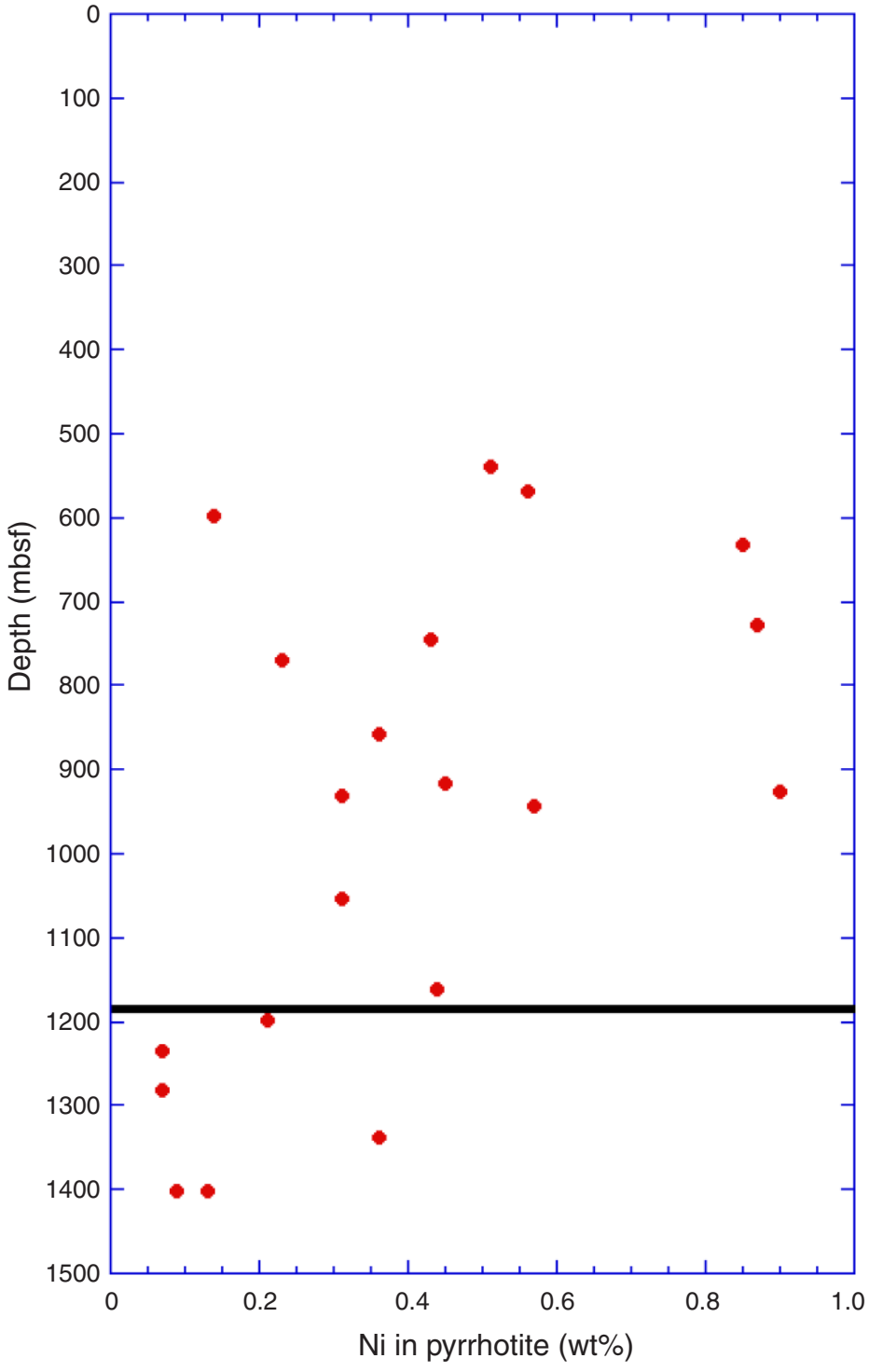

Figure F8. Ni in pentlandite is relatively constant downsection. The dark horizontal line marks the depth of this abrupt mineralogical and geochemical boundary.

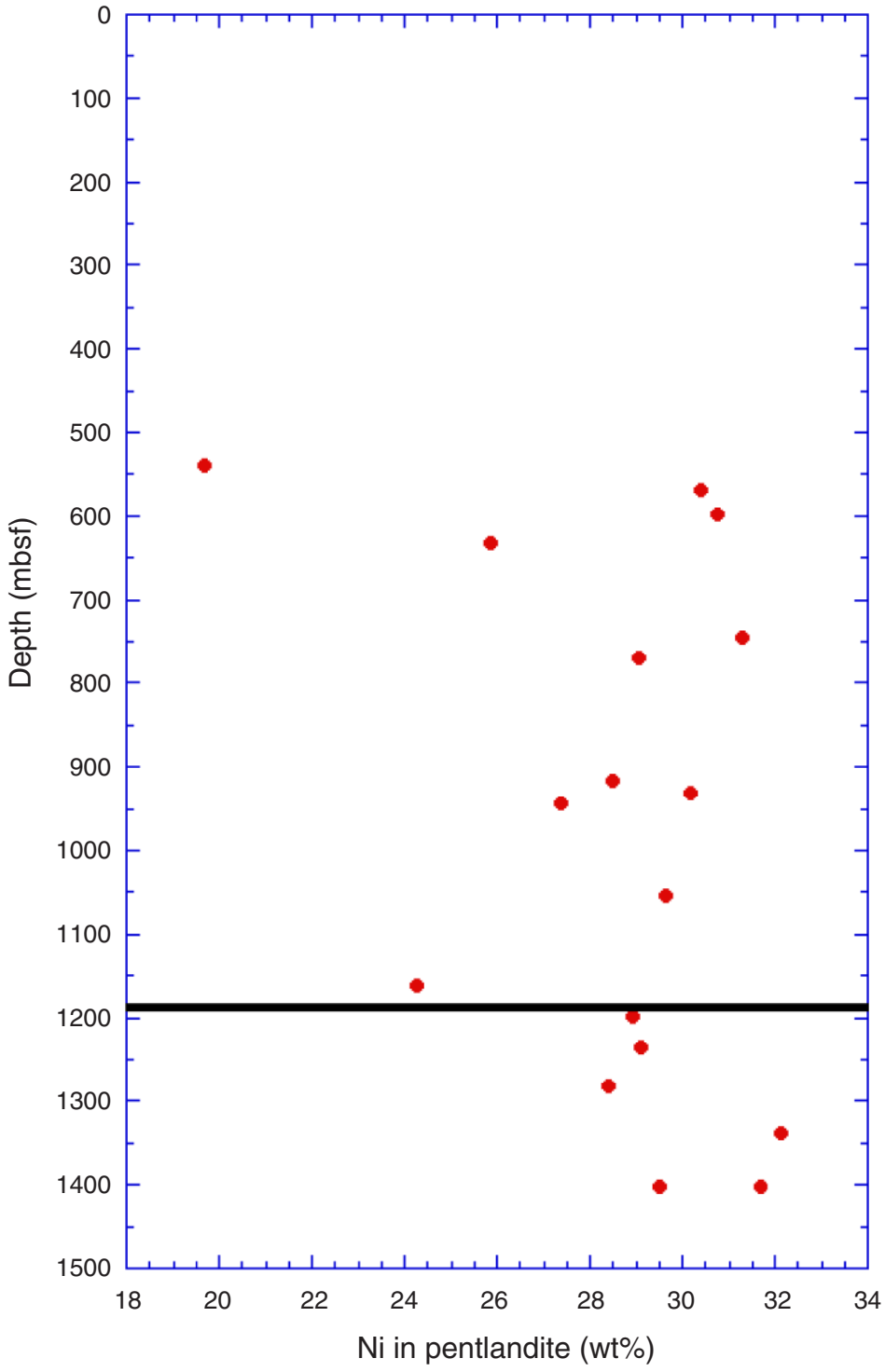

Figure F9. Co in pentlandite shows a sharp increase coincident with the base of Leg 176 lithologic unit X (dashed line at 954 mbsf) and a steady decrease in samples below our proposed lithologic unit boundary at between 1165 and 1190 mbsf). The dark horizontal line marks the depth of this abrupt mineralogical and geochemical boundary.

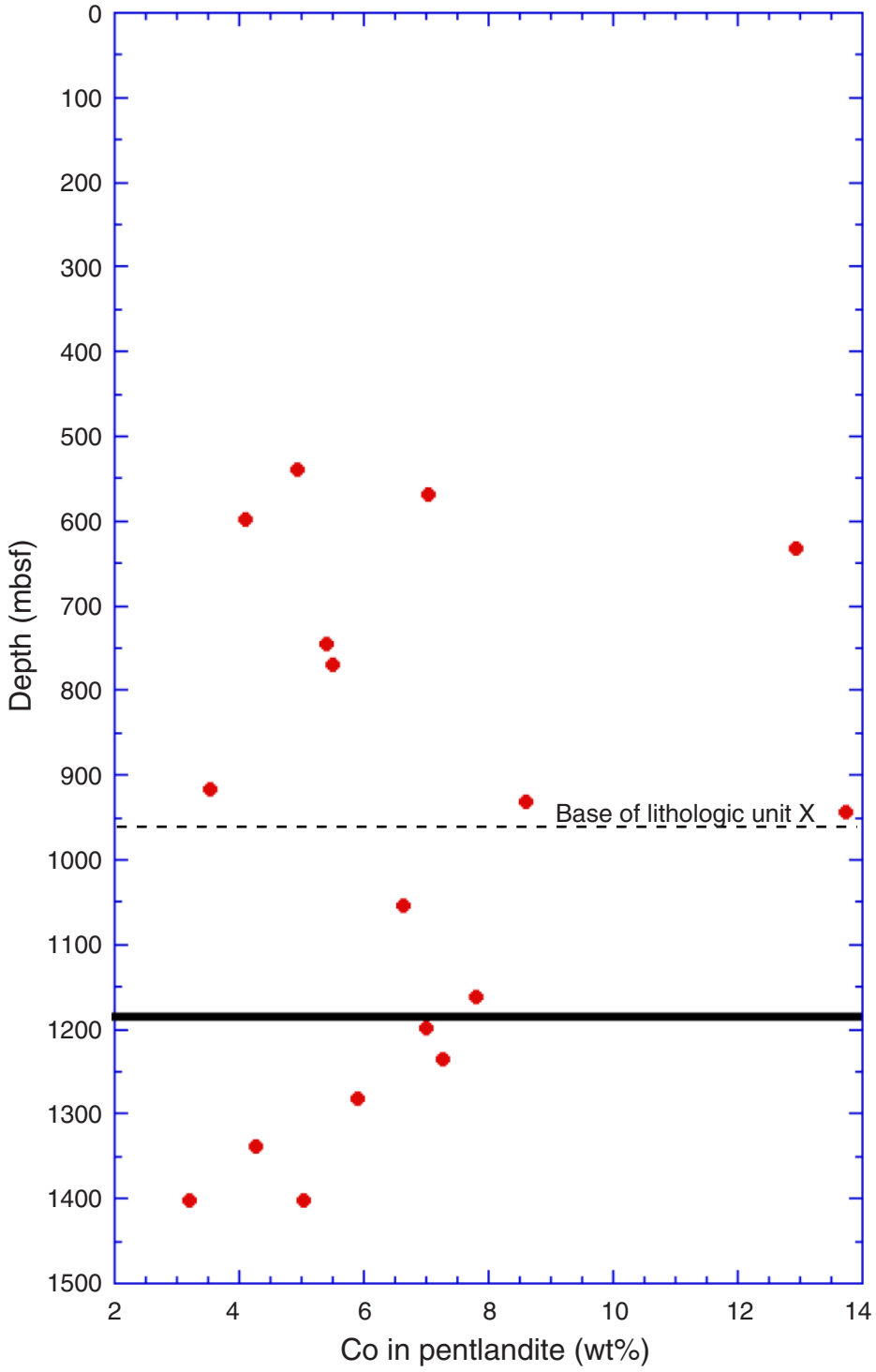

Figure F10. Plots vs. depth of bulk rock Ni and Cu compositions in samples from Hole 735B. Circles represent Ni compositions, and squares represent Cu compositions. Open symbols are from Leg 118 data (Robinson, Von Herzen, et al., 1989); solid symbols are from Leg 176 (Dick, Natland, Miller, et al., 1999) and this study.

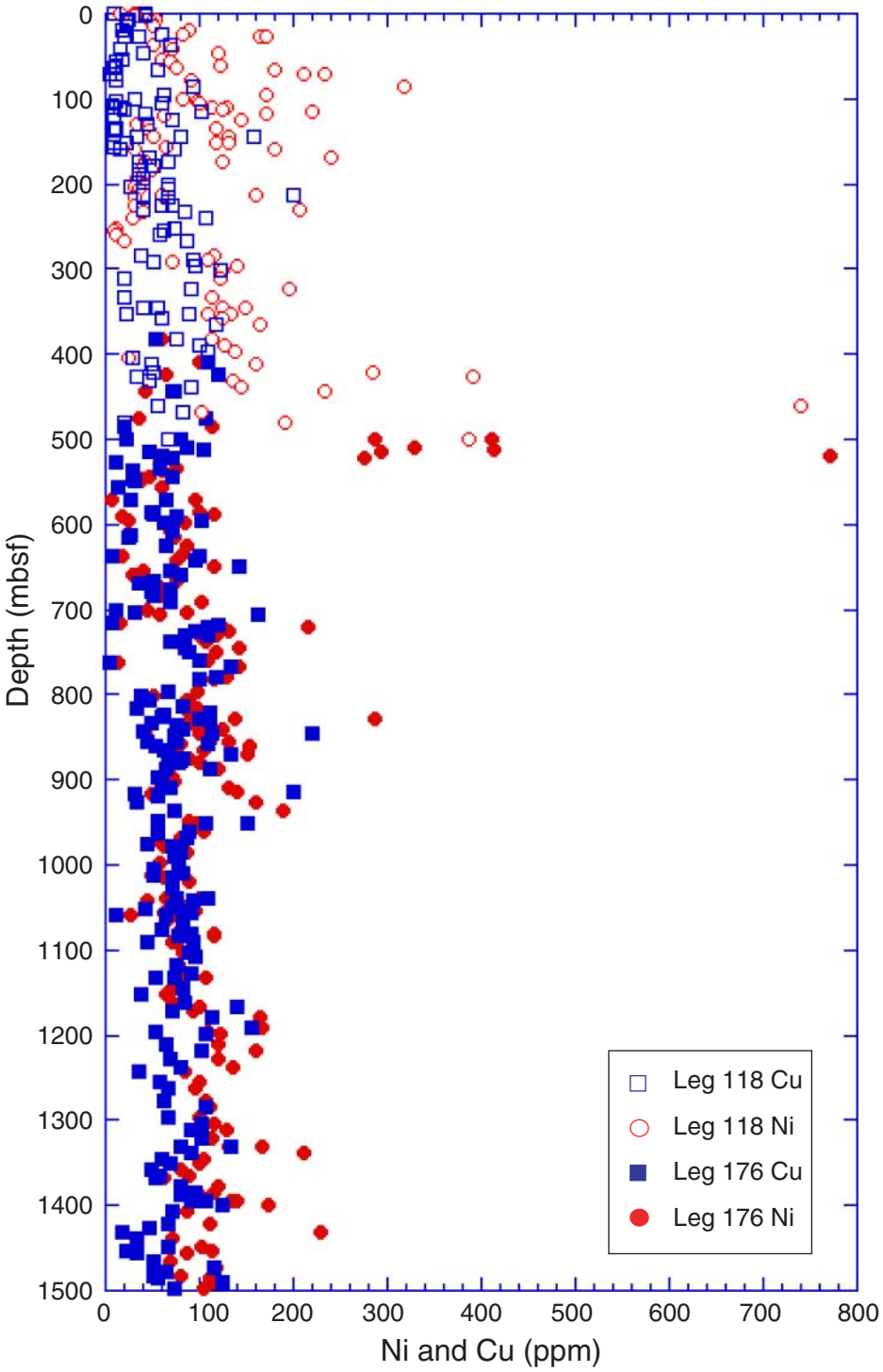

Figure F11. Covariation of bulk rock Ni and Cu in samples from Hole 735B. Open circles are data from olivine-bearing gabbros, solid squares are data from gabbros, and solid diamonds are data from oxide-bearing gabbros.

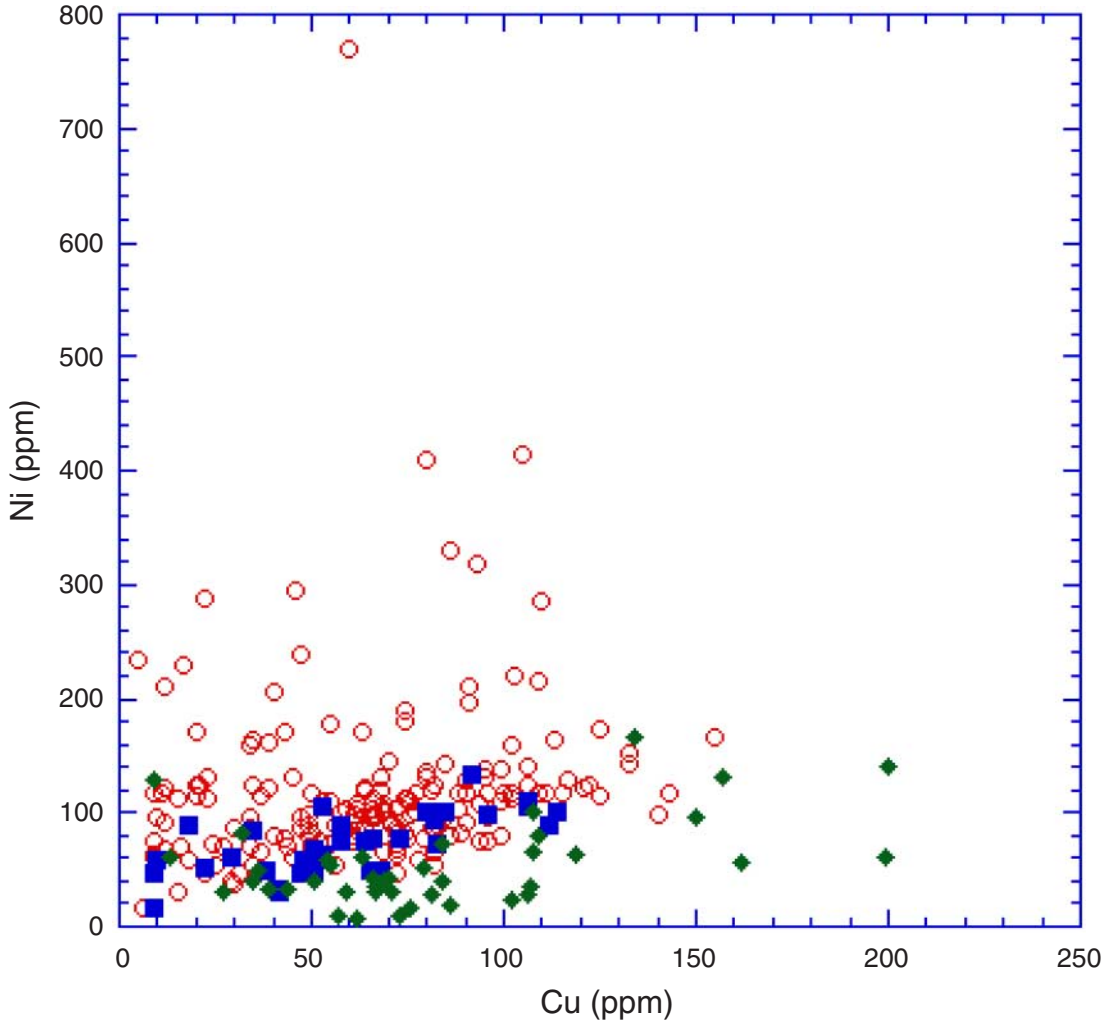

Figure F12. In this sample from the interval between 500 and 520 mbsf (Sample 176-735B-123R-4, 106–111 cm), pentlandite (brighter hue and softer) is much more abundant than pyrrhotite.

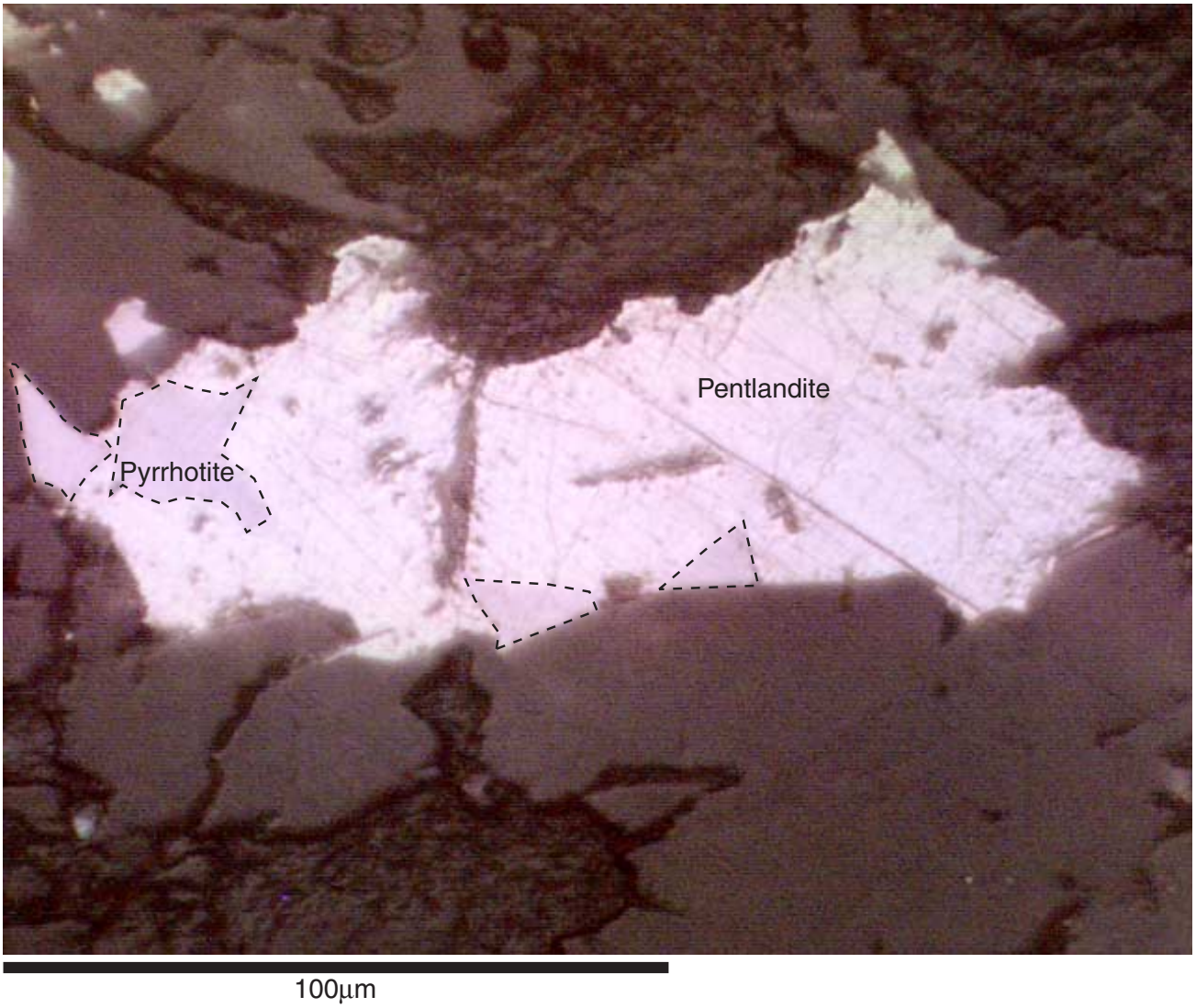

Table T1. Petrographic summaries of samples from Hole 735B. (See table note. Continued on next page.)

Core, section, interval (cm)	Description
176-735B-	
90R-1, 123–125	Medium coarse-grained, leucocratic olivine gabbro. 78% plagioclase, 12% clinopyroxene, 10% olivine, trace sulfides (po > tr > pn > cpy > py), trace oxides (sulfides > oxides), trace amphibole. Olivine <5% altered to smectite (50%), amphibole (40%), talc (5%), and magnetite (5%). Clinopyroxene and plagioclase <1% altered to amphibole.
90R-4, 42–45	Medium-grained, leucocratic olivine gabbro. 70% plagioclase, 15% clinopyroxene, 15% olivine, trace sulfides (po > pn > cpy), trace oxides (sulfides > oxides), trace amphibole. Olivine 30% altered to smectite (40%), amphibole (40%), talc (15%), and magnetite (5%). Clinopyroxene 20% altered to amphibole. Plagioclase 5% altered to amphibole.
90R-6, 72–77	Coarse-grained troctolite. 60% plagioclase, 35% olivine, 5% clinopyroxene, trace sulfides (po > tr > pn > cpy > py), trace oxides (sulfides > oxides), trace amphibole. Olivine 20% altered to amphibole (60%) smectite (20%), talc (15%), and magnetite (5%). Clinopyroxene 20% altered to amphibole. Plagioclase 5% altered to amphibole.
91R-1, 106–111	Medium-grained troctolite. 50% olivine, 45% plagioclase, 5% clinopyroxene, <1% sulfides (po > pn > cpy > py), trace oxides (sulfides > oxides). Olivine 5% altered to amphibole (80%), talc (15%), and magnetite (5%). Clinopyroxene 15% altered to amphibole, plagioclase 5% altered to amphibole.
101R-3, 82–87	Coarse-grained, oxide-bearing olivine gabbro. 55% plagioclase, 35% clinopyroxene, 8% olivine, 2% oxides (predominantly ilmenite), trace sulfides (po > cpy > pn > py). Olivine 15% altered to amphibole (90%), talc (5%), magnetite (5%). Clinopyroxene 10% altered to amphibole, plagioclase 5% altered to amphibole.
114R-1, 84–90	Coarse-grained, oxide gabbronorite. 45% plagioclase, 30% clinopyroxene, 15% orthopyroxene 10% oxides (predominantly ilmenite), <1% olivine, trace sulfides (po > cpy > py > pn). Olivine 40% altered to smectite (65%), amphibole (20%), talc 10%, magnetite (5%).
121R-6, 37–42	Coarse-grained oxide gabbro. 60% clinopyroxene, 35% plagioclase, 5% oxide, trace olivine,trace sulfides along grain boundaries (py > po > cpy > pn) intergrown with trace oxides and brown amphibole. Clinopyroxene 25% altered to amphibole.
123R-4, 106–111	Medium-grained, olivine gabbro. 55% plagioclase, 35% clinopyroxene, 10% olivine, trace sulfides (common along grain boundaries, tr > po > cpy > pn > py). Olivine 5% altered to smectite (60%), amphibole (35%), magnetite (5%). Plagioclase and clinopyroxene only slightly altered (2%) to amphibole.
124R-1, 48–53	Medium- to coarse-grained olivine gabbro. 55% plagioclase, 35% clinopyroxene, 10% olivine, trace oxides and sulfides (po > cpy > pn > py). Olivine 5% altered to smectite (60%) amphibole (35%), and magnetite. Plagioclase and clinopyroxene 23% altered to amphibole.
127R-3, 113–117	Coarse-grained oxide and orthopyroxene bearing olivine gabbro. 50% plagioclase, 30% clinopyroxene, 10% olivine, 3% oxides, 2% orthopyroxene. Olivine 5% altered to amphibole > smectite > talc > magnetite. Clinopyroxene and plagioclase <2% altered to amphibole. Trace sulfides (po > cpy > pn > py).
132R-1, 107–112	Leucocratic oxide and olivine bearing gabbro. 80% plagioclase, 15% clinopyroxene, 3% oxides, 2% olivine, trace sulfides (po > cpy > pn > py). Olivine 30% altered (70% amphibole, 15% smectite, 10% talc, and 5% magnetite). Clinopyroxene 10% altered to amphibole, plagioclase 2% altered to amphibole.
133R-5, 82–87	Coarse-grained olivine gabbro. 25% olivine, 15% plagioclase, 60% clinopyroxene, trace oxides and sulfides (po > cpy > pn > py). Olivine is 10% altered to smectite with minor (<10%) magnetite. Clinopyroxene is 5% altered to amphibole, plagioclase is<1% altered to amphibole.
134R-5, 70–75	Coarse-grained olivine gabbro. 50% plagioclase, 30% clinopyroxene, 20% olivine, trace oxides > sulfides (tr > po > cpy > pn > py). Olivine 5% altered to smectite (85%), magnetite (10%), and amphibole (5%). Clinopyroxene 3% altered to amphibole, plagioclase <1% altered to amphibole.
137R-3, 126–130	Medium-grained olivine gabbro. Plagioclase 60%, clinopyroxene 25%, olivine 15%, trace sulfides (po > cpy > pn > py) and oxides. Olivine 5% altered to smectite (60%), amphibole (35%), and magnetite (5%). Clinopyroxene 5% altered to amphibole, plagioclase 1% altered to amphibole.
137R-6, 52–58	Medium coarse-grained olivine bearing oxide gabbronorite. 55% plagioclase, 25% clinopyroxene, 13% orthopyroxene, 5% oxides, 2% olivine, trace sulfides (po > cpy > py). Olivine 30% altered to talc (50%) and magnetite (50%) with minor smectite and amphibole. Orthopyroxene 20% altered to amphibole, clinopyroxene 10% altered to amphibole, plagioclase 1% altered to amphibole.
138R-7, 48–53	Medium-grained oxide bearing olivine gabbro. 52% plagioclase, 37% clinopyroxene, 10% olivine, 1% oxides, trace sulfides (po > cpy > pn > py). Olivine 5% altered to smectite (50%), magnetite (30%), amphibole (10%), and minor talc. Clinopyroxene 5% altered to amphibole, plagioclase 1% altered to amphibole.
140R-4, 34–40	Coarse-grained olivine gabbro. 40% plagioclase, 50% clinopyroxene, 10% olivine, trace oxides and sulfides (po > cpy > pn > py). Only trace alteration of olivine to smectite, amphibole, and magnetite, and trace alteration of clinopyroxene and plagioclase to amphibole.
144R-1, 145–150	Orthopyroxene bearing oxide gabbro. 50% Clinopyroxene, 40% plagioclase, 7% oxides, 3% orthopyroxene,<1% sulfides (po > py > cpy > pn). Pyroxenes are 10% altered to amphibole, plagioclase is 5% altered to amphibole.
144R-4, 66–71	Oxide bearing olivine gabbro. 52% plagioclase, 40% clinopyroxene, 7% olivine, 1% oxides, trace sulfides (po > cpy > pn > py). Olivine is 3% altered to smectite (60%), amphibole (30%) and magnetite (10%). Plagioclase and pyroxene are 3% altered to amphibole.
146R-3, 102–107	No section made. From a 10-m thick lithologic interval of coarse-grained olivine gabbro. Sample 176-735B-146R-4, 118–112 cm, is from 2 m lower in the same lithologic interval.
146R-4, 118–122	Coarse-grained olivine gabbro. 52% plagioclase, 35% clinopyroxene, 13% olivine, trace oxides and sulfides (po > cpy > pn > py). Olivine is slightly altered (2%) to smectite (60%), amphibole (30%), and magnetite (10%). Pyroxene and plagioclase are slightly altered 2% to amphibole.
147R-4, 6–15	Medium- to coarse-grained oxide bearing olivine gabbro. Plagioclase 64%, clinopyroxene 14%, olivine 20%, oxides 2%, trace sulfides (po > cpy > pn > py). Oxide occurs in clusters as matrix surrounding rounded clinopyroxene crystals. Olivine <1% altered to smectite (80%) and magnetite (10%), clinopyroxene partially recrystallized but <2% altered to amphibole. Plagioclase <1% altered to amphibole.
147R-6, 45–51	Medium-grained olivine gabbro. 64% plagioclase, 27% clinopyroxene, 8% olivine, trace oxides and rare sulfides (py > po > cpy). Olivine is slightly altered (2%) to smectite (95%) and magnetite (5%). Clinopyroxene is slightly (2%) altered to amphibole. Plagioclase is, for the most part, recrystallized and slightly altered (2%) to amphibole.

Table T1 (continued).

Core, section, interval (cm)	Description
159R-1, 121–125	Coarse-grained olivine gabbro. 54% plagioclase, 40% clinopyroxene, 6% olivine, trace oxides and sulfides (po > cpy > py > pn). Olivine 5% altered to amphibole (90%), smectite (5%), magnetite (5%), and minor talc. Clinopyroxene 5% altered to amphibole, plagioclase 1% altered to amphibole.
171R-3, 62–67	Medium-grained oxide and olivine bearing gabbro. 48% plagioclase, 47% clinopyroxene, 4% olivine, 1% oxides, trace sulfides (po > cpy > pn > py). Olivine 3% altered to smectite (65%), amphibole (30%), and magnetite (5%). Clinopyroxene 5% altered to amphibole, plagioclase 1% altered to amphibole.
173R-2, 108–113	Coarse-grained olivine gabbro. 60% plagioclase, 25% clinopyroxene, 15% olivine, trace oxides and sulfides (po > cpy > pn > py). Olivine 10% altered to smectite (90%), amphibole (5%), and magnetite (5%). Clinopyroxene 5% altered to amphibole, plagioclase 1% altered to amphibole.
175R-1, 87–92	Coarse-grained olivine gabbro. 60% plagioclase, 30% clinopyroxene, 10% olivine, trace oxides and sulfides (po > cpy > pn > py). Olivine 2% altered to smectite with traces of amphibole and magnetite. Clinopyroxene and plagioclase <1% altered to amphibole.
175R-1, 115–120	Coarse-grained oxide bearing olivine gabbro. 55% plagioclase, 35% clinopyroxene, 8% olivine, 2% oxides, trace sulfides (po > cpy > py > pn). Oxides commonly occur as vermicular intergrowths with altered olivine (10% to amphibole 50%, smectite 20%, magnetite 20%). Plagioclase and clinopyroxene 2% altered to amphibole.
189R-5, 1–4	Fine- to medium-grained olivine gabbro. 55% plagioclase, 38% clinopyroxene, 7% olivine, trace oxides and sulfides (tr > po > cpy > pn > py). Olivine trace alteration to smectite and minor magnetite. Plagioclase and pyroxene virtually fresh, only a trace of alteration to amphibole.
191R-2, 2–7	Contact between medium-grained olivine gabbro and coarse-grained gabbro. Olivine gabbro contains 55% plagioclase, 30% clinopyroxene, 15% olivine, and a trace of oxides and sulfides with po > cpy > pn > py. Olivine is 10% altered to smectite (80%), amphibole (10%), and magnetite (5%). Clinopyroxene is 10% altered to amphibole, plagioclase 1% altered to amphibole. Gabbro contains 60% plagioclase and 40% clinopyroxene with the same sulfide assemblage. Oxides are a higher proportion of opaques in olivine gabbro, sulfides are a higher proportion in gabbro. Clinopyroxene in gabbro is 40% altered to amphibole, but varies from nil to 100% in different crystals. Plagioclase is 5% altered to amphibole, particularly where in contact with altered clinopyroxene.
199R-6, 115–120	Coarse-grained olivine gabbro. 55% plagioclase, 32% clinopyroxene, 8% olivine, 0.5% oxides and a trace of sulfides (po > cpy > py). Olivine is 5% altered to smectite (80%), amphibole, (15%), and magnetite (5%). Clinopyroxene and plagioclase show a trace of alteration to amphibole.
200R-1, 12–16	Coarse-grained olivine gabbro. 35% plagioclase, 30% clinopyroxene, 35% olivine, trace oxides and sulfides (po > cpy > pn > py) but higher abundance of cpy and pn than most other samples. Olivine 5% altered to amphibole (70%), smectite (25%), and magnetite (1%). Clinopyroxene 2% altered to amphibole, plagioclase <1% altered to amphibole.
201R-5, 9–16	Coarse-grained gabbro. 65% plagioclase, 35% clinopyroxene, trace oxides and sulfides (po > pn > cpy > py) and sulfides > oxides. Clinopyroxene and plagioclase 5% altered to amphibole with minor smectite.
203R-1, 11–13	Coarse-grained oxide and sulfide bearing clinopyroxenite (po > cpy > pn). Sulfides and oxides are ameoboid clusters randomly distributed between the rounded edges of clinpyroxene grains and in this section sulfides are 3–4 modal percent of the rock. An adjacent billet has no visible sulfides, and this section could have been cut to show an even higher abundance of sulfides.
207R-1, 18–24	Medium- to fine-grained olivine gabbro. 60% plagioclase, 35% clinopyroxene, 5% olivine, trace of oxides and sulfides (po > cpy > pn > py). Olivine 20% altered to smectite (70%), amphibole (20%), talc (5%), and magnetite (5%). Plagioclase and clinopyroxene 1% altered to amphibole.
210R-4, 60–63	Coarse-grained olivine gabbro. 40% plagioclase, 45% clinopyroxene, 15% olivine. Trace oxides and sulfides (po > cpy > pn > py). Olivine 10% altered to smectite (85%), amphibole (10%), magnetite (5%). Clinopyroxene 5% altered to amphibole, plagioclase 1% altered to amphibole.

Note: tr = troilite, po = pyrrhotite, pn = pentlandite, cpy = chalcopyrite, py = pyrite.

Table T2. Sulfide mineral analyses, Hole 735B.

	Core, section	Depth (mbsf)	S (wt%)	Fe (wt%)	Cu (wt%)	Zn (wt%)	Ni (wt%)	Co (wt%)	Total (wt%)
	176-735B-								
Pyrrhotite	94R-3	540.28	39.37	59.86	0.02	0.01	0.51	0.01	99.77
	99R-3	569.83	39.28	59.65	0.05	0.04	0.56	0.02	99.60
	103R-3	599.06	39.49	59.78	0.02	0.01	0.14	0.03	99.48
	109R-3	631.58	38.69	58.70	0.01	0.02	0.85	0.13	98.41
	121R-6	727.08	38.75	59.70	0.03	0.01	0.87	0.16	99.53
	123R-4	744.24	39.30	59.58	0.01	0.01	0.43	0.00	99.34
	127R-3	768.75	39.12	59.96	0.01	0.02	0.23	0.00	99.33
	137R-6	858.84	38.91	59.38	0.02	0.00	0.36	0.05	98.72
	144R-4	917.09	39.01	59.20	0.03	0.01	0.45	0.00	98.70
	145R-4	926.40	39.39	59.25	0.02	0.01	0.90	0.12	99.68
	146R-1	931.64	39.23	59.83	0.01	0.01	0.31	0.01	99.40
	147R-4	944.46	39.32	58.98	0.03	0.01	0.57	0.09	99.00
	159R-1	1054.91	39.46	59.67	0.02	0.01	0.31	0.00	99.48
	171R-3	1162.57	39.29	59.89	0.01	0.00	0.44	0.02	99.64
	176R-2	1199.15	37.55	61.84	0.01	0.03	0.21	0.00	99.64
	180R-5	1236.49	36.85	61.85	0.01	0.02	0.07	0.00	98.79
	185R-3	1282.27	37.12	62.41	0.00	0.00	0.07	0.00	99.60
	191R-2	1337.22	38.57	60.67	0.01	0.02	0.36	0.00	99.63
	199R-6	1400.78	37.21	62.08	0.01	0.02	0.13	0.00	99.44
	200R-1	1402.12	37.53	61.84	0.03	0.01	0.09	0.00	99.49
Chalcopyrite	94R-3	540.28	34.71	29.77	34.47	0.05	0.01	0.00	99.01
	99R-3	569.83	34.60	30.01	34.05	0.23	0.05	0.02	98.95
	103R-3	599.06	34.84	30.20	34.27	0.04	0.01	0.00	99.36
	109R-3	631.58	34.76	29.92	33.63	0.06	0.04	0.00	98.41
	114R-1	653.24	34.72	29.58	34.21	0.05	0.01	0.00	98.57
	121R-6	727.08	34.78	29.66	34.42	0.06	0.01	0.00	98.92
	123R-4	744.24	34.85	29.88	34.38	0.02	0.03	0.00	99.17
	127R-3	768.75	34.51	29.87	34.16	0.16	0.28	0.01	98.99
	137R-6	858.84	34.83	29.90	33.65	1.15	0.01	0.00	99.53
	144R-4	917.09	34.25	30.22	34.31	0.01	0.02	0.00	98.81
	145R-4	926.40	34.70	29.69	34.36	0.03	0.01	0.00	98.79
	146R-1	931.64	34.74	29.68	34.23	0.02	0.01	0.00	98.67
	147R-4	944.46	34.83	29.58	34.06	0.03	0.01	0.00	98.51
	159R-1	1054.91	34.81	29.83	34.14	0.03	0.02	0.00	98.84
	171R-3	1162.57	34.83	29.86	34.29	0.04	0.01	0.00	99.02
	176R-2	1199.15	34.91	29.85	34.20	0.05	0.01	0.00	99.01
	180R-5	1236.49	34.84	29.91	34.48	0.02	0.02	0.00	99.26
	185R-3	1282.27	34.72	30.03	33.78	0.00	0.47	0.14	99.13
	191R-2	1337.22	34.93	29.80	34.25	0.04	0.01	0.00	99.03
	199R-6	1400.78	34.99	29.94	34.34	0.03	0.02	0.00	99.32
	200R-1	1402.12	34.97	30.17	34.40	0.02	0.02	0.00	99.58
Pentlandite	94R-3	540.28	36.15	38.72	0.00	0.00	19.70	4.94	99.51
	99R-3	569.83	33.11	29.23	0.02	0.01	30.42	7.03	99.82
	103R-3	599.06	34.06	30.16	0.26	0.08	30.77	4.10	99.42
	109R-3	631.58	33.33	27.31	0.02	0.05	25.87	12.93	99.49
	123R-4	744.24	33.24	29.67	0.00	0.00	31.31	5.41	99.63
	127R-3	768.75	33.39	31.71	0.02	0.00	29.08	5.51	99.71
	144R-4	917.09	33.89	30.98	3.19	0.02	28.47	3.55	100.09
	146R-1	931.64	33.16	27.79	0.11	0.00	30.17	8.61	99.84
	147R-4	944.46	33.42	25.39	0.00	0.04	27.39	13.74	99.97
	159R-1	1054.91	33.31	29.77	0.00	0.00	29.66	6.63	99.36
	171R-3	1162.57	34.17	33.61	0.00	0.00	24.26	7.81	99.85
	176R-2	1199.15	33.42	30.20	0.01	0.04	28.92	6.99	99.56
	180R-5	1236.49	33.40	29.86	0.03	0.00	29.13	7.28	99.68
	185R-3	1282.27	33.37	31.98	0.14	0.01	28.42	5.91	99.83
	191R-2	1337.22	33.46	30.31	0.01	0.01	32.14	4.28	100.21
	199R-6	1400.78	33.28	31.32	0.00	0.00	31.67	3.21	99.49
	200R-1	1402.12	33.27	31.65	0.12	0.01	29.50	5.03	99.58
Pyrite	94R-3	540.28	53.07	46.07	0.00	0.03	0.02	0.01	99.21
	99R-3	569.83	53.33	45.52	0.02	0.00	0.38	0.21	99.45
	114R-1	653.24	52.80	45.83	0.02	0.02	0.31	0.17	99.14
	146R-1	931.64	53.20	46.79	0.00	0.01	0.01	0.00	100.00
Sphalerite	180R-5	1236.49	33.81	10.19	0.38	55.09	0.03	0.14	99.64

Table T3. Bulk rock chemistry of samples, Hole 735B. (Continued on next two pages.)

Leg, hole:	176-735B-																
Core:	90R*	90R*	90R	91R*	101R	114R	121R	123R	124R	127R	132R	133R*	134R	137R*	137R	138R	140R
Section:	1	4	6	1	3	1	6	4	1	3	1	5	5	3	6	7	4
Piece:	2	1	4A	3	1G	6B	1C	3	2B	6	12	2	1B		1D	2	2
Interval (cm):	123–125	42–45	72–77	106–111	82–87	84–90	37–42	106–111	48–53	113–117	107–112	82–87	70–75	126–130	52–58	48–53	34–40
Depth (mbsf):	509.03	512.41	515.23	518.46	588.44	653.24	727.08	744.24	749.18	768.75	814.27	829.28	838.81	855.38	858.84	870.00	884.56
Major element oxides (wt%):																	
SiO_2	48.10	48.42	45.15	43.82	49.01	46.42	49.03	50.42	49.93	49.56	50.88	50.47	48.90	51.88	51.13	52.01	49.93
TiO_2	0.11	0.10	0.17	0.15	0.46	4.26	0.58	0.45	0.46	0.33	0.94	0.40	0.46	0.35	0.45	0.61	0.63
Al_2O_3	22.05	18.01	17.78	13.37	14.85	12.55	14.34	15.60	15.52	17.70	7.43	5.91	13.97	18.26	16.09	12.67	14.77
Fe_2O_3	5.35	5.64	6.78	9.41	8.34	16.05	7.93	6.76	6.74	6.21	9.78	10.15	9.29	7.36	6.44	5.65	7.95
MnO	0.09	0.09	0.10	0.14	0.17	0.25	0.14	0.13	0.12	0.12	0.23	0.18	0.15	0.13	0.13	0.14	0.14
MgO	11.39	14.77	16.21	24.03	10.68	6.28	10.92	10.28	10.50	9.24	12.64	21.80	12.65	10.74	8.86	10.17	10.84
CaO	11.27	11.83	9.43	7.94	12.36	10.32	13.28	13.09	13.53	12.57	16.05	14.03	11.86	12.05	13.53	15.37	12.52
Na_2O	2.40	1.67	1.95	1.08	2.60	3.26	2.52	2.63	2.66	2.97	1.52	0.73	2.40	2.89	2.83	2.37	2.58
K_2O	0.01	0.20	0.17	0.01	0.14	0.08	0.06	0.08	0.04	0.08	0.06	0.00	0.04	0.03	0.05	0.07	0.06
P_2O_5	0.01	0.00	0.04	0.01	0.01	0.04	0.05	0.01	0.03	BDL	BDL	0.01	0.01	0.09	0.07	0.04	0.04
C			0.02		0.05	0.02	0.21	0.04	0.02	0.01	0.01		0.01		0.01	0.02	0.02
S			0.05		0.03	0.19	0.09	0.03	0.05	0.04	0.07		0.1		0.07	0.02	0.05
Total	100.76	100.72	100.05	99.95	99.90	100.02	100.15	99.92	99.90	99.93	100.05	103.66	99.94	103.76	100.06	99.94	99.93
LOI	0.0	0.0	2.2	0.0	1.2	0.3	1.0	0.4	0.3	1.1	0.4	0.0	0.1	0.0	0.4	0.8	0.4
Mg#	0.83	0.86	0.85	0.86	0.75	0.48	0.76	0.78	0.78	0.78	0.75	0.83	0.76	0.77	0.76	0.81	0.76
Ca#	0.72	0.80	0.73	0.80	0.72	0.64	0.74	0.73	0.74	0.70	0.85	0.91	0.73	0.70	0.73	0.78	0.73
Trace elements (ppm):																	
V	38	71		48								220		99			
Cr	228	1202	129	742	156	27	184	326	136	116	170	1003	156	153	245	170	156
Ni	329	413	396	770	113	33	115	96	95	103	76	286	153	131	110	49	108
Cu	86	105	68	60	77	52	78	55	82	59	49	110	108	45	34	36	61
Zn	33	47	49	52	BDL	133	BDL	89	BDL	40	55	55	51	49	BDL	BDL	96
Rb	1	2		2								0		2			
Sr	184	135	148	109	168	163	152	159	161	169	74	45	147	180	167	137	152
Y	5	6	BDL	5	11	29	12	10	11	BDL	25	11	10	14	BDL	21	11
Zr	21	21	BDL	15	22	80	20	24	20	BDL	30	19	28	72	BDL	53	13
Nb	1	1	BDL	0	BDL	BDL	BDL	BDL	BDL	BDL	BDL	0	BDL	0	BDL	BDL	BDL
Ba			BDL		6	5	7	5	6	BDL	BDL		BDL		BDL	BDL	BDL
Co			59		45	33	42	36	35	31	38		54		30	29	38
Ce			BDL		BDL	BDL	BDL	BDL	BDL	BDL	BDL		BDL		BDL	BDL	BDL
Sc			7		35	45	47	40	45	34	83		37		39	58	39
Ta			BDL		BDL	BDL	BDL	BDL	BDL	BDL	BDL		BDL		BDL	BDL	BDL
Pd (ppb):	0.618	0.779	0.265	0.271	BDL	BDL	0.327	1.890	0.148	BDL	0.129	0.054	BDL	0.083	0.093	0.192	0.164
Pt (ppb):	0.543	0.267	0.160	0.208	BDL	0.041	BDL	0.376	BDL	BDL	BDL	BDL	BDL	BDL	BDL	BDL	BDL
Ir (ppb):	0.026	0.013	0.005	0.114	0.008	0.008	BDL	0.028	0.006	0.005	BDL	0.006	BDL	0.009	BDL	BDL	0.005
Ru (ppb):	0.069	0.060	0.026	0.426	BDL	BDL	BDL	0.171	BDL	BDL	BDL	BDL	BDL	BDL	BDL	BDL	BDL
Rh (ppb):	0.020	0.022	0.007	0.023	0.004	0.022	0.046	0.099	0.049	0.010	0.007	0.015	0.012	0.007	0.007	0.007	0.054
Au (ppb):	0.271	0.796	0.786	0.463	0.217	0.309	0.145	0.270	0.309	0.175	0.284	0.094	0.258	0.105	0.499	BDL	0.405

Notes: * = BDL. Blank cell = not in analytical suite. BDL = below detection limit. Ca# = Molar Ca/Ca+Na. LOI = loss on ignition.

Table T3 (continued).

Leg, hole:	176-735B-																
Core:	144R*	144R	146R	146R*	147R	147R*	159R	171R	173R	175R*	175R	189R*	191R	199R	200R	201R	203R
Section:	1	4	3	4	4	6	1	3	2	1	1	5	2	6	1	5	1
Piece:	3	2A	3	3	1A	2	9	3A	4	4	5	1	1	6	2	1	1
Interval (cm):	145–150	66–71	102–107	120–123	6–15	47–51	121–125	62–67	108–113	87–92	115–120	0–5	2–7	115–120	12–16	9–16	11–13
Depth (mbsf):	913.75	917.09	934.76	936.34	944.46	947.41	1054.91	1162.57	1180.98	1191.97	1192.25	1322.12	1337.22	1400.78	1402.12	1416.75	1430.91
Major element oxides (wt%):																	
SiO_2	49.52	51.88	48.57	49.21	46.65	51.56	51.57	50.86	48.35	49.52	51.21	52.53	52.73	49.09	45.45	51.42	46.74
TiO_2	2.15	0.56	0.43	0.52	1.69	0.59	0.52	0.77	0.74	0.31	0.64	0.27	0.37	0.27	0.28	0.44	1.47
Al_2O_3	8.45	14.85	12.92	15.16	4.02	16.97	16.11	13.99	18.17	15.43	16.48	17.12	18.19	17.51	9.54	17.37	6.10
Fe_2O_3	14.36	5.20	9.25	8.44	16.06	7.78	6.74	7.90	9.01	7.35	6.69	6.25	5.10	7.09	13.89	4.81	15.38
MnO	0.27	0.12	0.16	0.14	0.35	0.14	0.14	0.16	0.13	0.13	0.14	0.12	0.11	0.12	0.22	0.10	0.27
MgO	10.77	8.89	13.82	12.87	15.13	8.72	8.19	9.71	10.32	11.30	8.64	9.89	6.57	11.00	20.91	7.93	12.33
CaO	13.36	15.08	12.26	11.90	15.08	11.86	12.16	13.20	9.56	12.15	12.82	13.93	12.55	11.19	8.00	14.02	14.89
Na_2O	1.82	2.68	2.10	2.27	0.84	3.12	3.40	2.65	3.06	2.49	2.90	2.60	3.48	2.82	1.57	2.88	1.39
K_2O	0.04	0.06	0.08	0.02	0.04	0.05	0.09	0.07	0.07	0.02	0.06	0.01	0.09	0.05	0.05	0.05	0.07
P_2O_5	0.08	0.04	0.04	0.03	0.04	0.03	0.10	0.05	0.10	0.02	0.03	0.00	0.02	0.06	0.02	0.04	0.21
C		0.01	0.01		0.03		0.11	0.02	0.01		0.01		0.02	0.02	0.02	0.01	0.01
S		0.02	0.04		0.19		0.03	0.1	0.08		0.08		0.13	0.08	0.08	0.06	1.86
Total	101.80	99.99	99.88	100.76	100.22	101.02	99.96	99.98	100.00	98.72	100.10	102.72	99.96	100.10	100.13	99.93	101.42
LOI	1.0	0.6	0.2	0.2	0.1	0.2	0.8	0.5	0.4	0.0	0.4	0.0	0.6	0.8	0.1	0.8	0.7
Mg#	0.64	0.80	0.78	0.78	0.69	0.72	0.74	0.74	0.73	0.78	0.75	0.79	0.75	0.78	0.78	0.79	0.65
Ca#	0.80	0.76	0.76	0.74	0.91	0.68	0.66	0.73	0.63	0.73	0.71	0.75	0.67	0.69	0.74	0.73	0.86
Trace elements (ppm):																	
V	441			137		147				138		164					
Cr	214	347	510	609	218	79	95	109	68	192	224	137	150	122	136	218	605
Ni	141	64	136	189	101	89	65	99	137	167	69	113	100	137	259	60	806
Cu	200	33	54	74	89	56	52	85	67	155	49	102	116	64	141	69	1214
Zn	92	BDL	126	57	58	59	BDL	119	BDL	48	BDL	34	BDL	BDL	23	44	53
Rb	0			0		1				0		0					
Sr	83	154	130	150	39	179	200	148	206	161	182	168	214	201	4-Oct	177	64
Y	45	14	BDL	12	49	16	24	24	BDL	9	16	5	17	BDL	BDL	10	86
Zr	85	20	11	41	77	44	545	46	29	33	19	15	34	BDL	16	BDL	146
Nb	1	BDL	BDL	2	BDL	2	BDL	BDL	BDL	1	BDL	1	BDL	BDL	BDL	BDL	BDL
Ba		BDL	5		BDL		7	BDL	BDL		BDL		5	BDL	BDL	BDL	6
Co		22	49		62		34	34	52		26		28	42	98	21	106
Ce		BDL	BDL		BDL		BDL	BDL	BDL		BDL		BDL	BDL	BDL	BDL	25
Sc		50	39		85		32	47	11		35		30	22	24	40	67
Ta		BDL	BDL		BDL		BDL	BDL	BDL		BDL		BDL	BDL	BDL	BDL	BDL
Pd (ppb):	BDL	BDL	BDL	BDL	0.086	0.121	0.125	0.140	0.216	0.349	BDL	0.244	0.236	BDL	BDL	0.052	46.700
Pt (ppb):	0.074	0.059	0.075	0.035	BDL	BDL	BDL	BDL	BDL	BDL	1.101	BDL	0.080	BDL	BDL	BDL	7.951
Ir (ppb):	0.016	0.012	0.005	0.052	0.017	0.006	0.009	0.007	BDL	0.009	BDL	0.019	BDL	BDL	0.014	BDL	1.090
Ru (ppb):	BDL	BDL	0.043	BDL	0.168	BDL	BDL	BDL	BDL	BDL	BDL	BDL	BDL	BDL	BDL	BDL	3.018
Rh (ppb):	0.033	0.050	0.043	0.019	0.060	0.013	0.049	0.048	0.046	0.014	0.059	0.019	0.053	0.043	0.059	0.033	1.664
Au (ppb):	0.092	0.230	0.424	0.188	0.084	0.140	0.103	0.129	0.107	0.140	0.179	BDL	0.230	0.178	0.136	0.205	BDL

Table T3 (continued).

Leg, hole:	176-735B-	
Core:	207R	210R
Section:	1	4
Piece:	1C	1
Interval (cm):	18–24	60–63
Depth (mbsf):	1469.68	1502.98
Major element oxides (wt%):		
SiO_2	49.09	52.79
TiO_2	0.39	0.39
Al_2O_3	15.66	15.29
Fe_2O_3	6.96	6.00
MnO	0.12	0.13
MgO	12.08	10.78
CaO	12.70	15.21
Na_2O	2.41	2.34
K_2O	0.04	0.01
P_2O_5	0.10	0.01
C	0.05	
S	0.08	
Total	99.68	102.95
LOI		
Mg#	0.80	0.81
Ca#	0.74	0.78
Trace elements (ppm):		
V		209
Cr	2054	196
Ni	105	97
Cu	140	47
Zn	BDL	33
Rb		2
Sr	158	147
Y	BDL	13
Zr	15	24
Nb	BDL	0
Ba	BDL	
Co	36	
Ce	BDL	
Sc	36	
Ta	BDL	
Pd (ppb):	0.072	0.109
Pt (ppb):	BDL	0.085
Ir (ppb):	0.005	0.017
Ru (ppb):	BDL	BDL
Rh (ppb):	0.042	0.004
Au (ppb):	0.499	BDL